



# Revisiting classical concepts of Linear Elastic Fracture Mechanics - Part I: The closing ‘mathematical’ crack in an infinite plate and the respective Stress Intensity Factors

Christos F. Markides

*National Technical University of Athens, School of Applied Mathematical and Physical Sciences, Department of Mechanics, Laboratory for Testing and Materials, Zografou Campus, 5 Heroes of Polytechnion Avenue, 157 73, Attiki, Greece*  
markidib@maill.ntua.gr, <http://orcid.org/0000-0001-6547-3616>

Stavros K. Kourkoulis

*National Technical University of Athens, School of Applied Mathematical and Physical Sciences, Department of Mechanics, Laboratory of Biomechanics and Biomedical Physics, Zografou Campus, 5 Heroes of Polytechnion Avenue, 157 73, Attiki, Greece*  
stakour@central.ntua.gr, <http://orcid.org/0000-0003-3246-9308>

**ABSTRACT.** This is the first part of a short three-paper series, aiming to revisit some classical concepts of Linear Elastic Fracture Mechanics. The motive of this first paper is to highlight some controversial issues, related to the unnatural overlapping of the lips of a ‘mathematical’ crack in an infinite plate loaded by specific combinations of principal stresses at infinity (predicted by the classical solution of the respective first fundamental problem), and the closely associated issue of negative mode-I Stress Intensity Factor. The problem is confronted by superimposing to the first fundamental problem of Linear Elastic Fracture Mechanics for an infinite cracked plate (with stress-free crack lips) an ‘inverse’ mixed fundamental problem. This superposition provides naturally acceptable stress and displacement fields, prohibiting overlapping of the lips (by means of contact stresses generated along the crack lips, which force the overlapped lips back to naturally accepted position) and, also, non-negative mode-I Stress Intensity Factors. The solutions of this first paper form the basis for the next two papers of the series, dealing with the respective problems in finite domains (recall, for example, the cracked Brazilian disc configuration) weakened by artificial notches (rather than ‘mathematical’ cracks), by far more interesting for practical engineering applications.

**KEYWORDS.** Linear Elastic Fracture Mechanics, ‘Mathematical’ cracks, Stress Intensity Factors, Stresses, Displacements and Contact stresses, Overlapping crack lips, Complex potentials.



**Citation:** Markides, Ch.F, Kourkoulis, S.K., Revisiting classical concepts of Linear Elastic Fracture Mechanics-Part I: The closing ‘mathematical’ crack in an infinite plate and the respective Stress Intensity Factors, *Frattura ed Integrità Strutturale*, 66 (2023) 233-260.

**Received:** 10.08.2023  
**Accepted:** 21.08.2023  
**Online first:** 26.08.2023  
**Published:** 01.10.2023

**Copyright:** © 2023 This is an open access article under the terms of the CC-BY 4.0, which permits unrestricted use, distribution, and reproduction in any medium, provided the original author and source are credited.

## INTRODUCTION

The rapid increase of computational power (either at the level of Super-Computers or at that of the Mainframes and the Personal Computers), which characterizes the last few decades, permitted the development of some quite flexible and efficient numerical tools (as it is, for example, the Finite Element Method), which are broadly applied nowadays worldwide, providing solutions (even of approximate nature) to some quite complicated problems of the Structural Engineering community. Among these problems, the ones related to the stress and displacement fields developed in cracked bodies, are typical examples. It is (or it appears to be) relatively easy to calculate the stresses and displacements developed in a three dimensional body of arbitrary geometry, weakened by a crack (or a network of cracks), under any complicated loading scheme. The closed-form analytical solution of such problems, by means of the tools and techniques of Linear Elastic Fracture Mechanics (LEFM) available in the hands of Engineers and Mathematicians, was almost impossible in most cases (obviously things are even more complicated in branches of Fracture Mechanics, in which the assumptions of Linear Elasticity are not acceptable, like, for example, the branch of Elastic-Plastic Fracture Mechanics).

As a consequence, the analytic investigation of such problems is gradually abandoned and attention is paid to numerical schemes, providing solutions for the stress and displacement fields according to a fast manner, permitting, also, detailed parametric studies. However, even the simplest numerical models need proper validation and calibration before they can be considered as reliable tools of practical value. Validation is usually achieved by considering the solution of some classes of problems (i.e., for a specific set of parameters) against the data obtained from properly designed experimental protocols. Unfortunately, in many cases it is difficult (or very expensive in terms of time and resources) to implement laboratory protocols simulating accurately enough the conditions of the actual problem that is planned to be solved numerically. As a result, one is often forced to resort to analytical solutions, even for a special (simple) case of the general problem. Therefore, it is quite possible that the traditional (even not very modern) tools of LEFM to be proven extremely valuable.

In this context, an attempt is undertaken in this study to revisit some classical concepts of LEFM and shed light to a few controversial issues, concerning the Structural Engineering community since many years. The study is described in a short series of three-papers. In this first part of the series, attention is paid to the infinite plate with a ‘mathematical’ crack. The term ‘mathematical’ crack is used to describe a discontinuity in the form of a straight crack the lips of which are at zero distance from each other. Obviously, the concept of a ‘mathematical’ crack is of limited practical importance and the same is true for the concept of an infinite plate. However, the importance of the issues that will be discussed in this first paper lies to that they form the basis for the remaining two papers, in which stress and displacement fields will be determined in bodies of finite dimensions, weakened by discontinuities in the form of notches, i.e., discontinuities without a singular tip (or, in other words, configurations for which the traditional definition of the Stress Intensity Factor (SIF) is not any longer adequate and it is, therefore, substituted by the concept of the Notch Stress Intensity Factor (NSIF) [1-4].

The issues that will be considered in this first paper are related to the contact stresses inevitably generated along the lips of a ‘mathematical’ crack, in an infinite plate that is subjected to specific combinations of principal stresses at infinity. These stresses (generated along loci which are initially assumed to be stress free) prohibit the unnatural overlapping of the crack lips provided by the classical solution of the respective first fundamental problem of LEFM. Closely associated to these contact stresses is the issue of negative values for the mode-I SIF, which is generally obtained in case the solution of the respective first fundamental problem of LEFM is mechanically applied to the definition of the respective SIFs.

As it was already highlighted, the above issues concerned long ago the community of Fracture Mechanics and have been studied in-depth already since the late sixties, in conjunction with the problem of the partially closed Griffith crack [5-10]. It is to be clarified here that overlapping of crack lips is not a naturally observable phenomenon but rather it is just an inherent inability of LEFM to accurately depict reality for the specific problem. Indeed, according to the classical solution of LEFM, for an infinite plate loaded at infinity and weakened by a ‘mathematical’ crack with stress-free lips, both the opening and the overlapping of the crack lips are possible to appear. However, it is obvious that the non-zero thickness of the plate prohibits overlapping. In other words, while crack closure is an observable phenomenon (accompanied by generation of contact stresses, which alter the initially adopted boundary conditions), overlapping of the crack lips is an unnatural phenomenon, which must be properly addressed by somehow reconsidering the classical solution of LEFM.

It was Bowie and Freese [11], who confronted for the first time the problem of overlapping for an infinite plate with an internal ‘mathematical’ crack, assuming that the plate was subjected to in-plane bending. They assumed that an acceptable (from the physical point of view) solution is obtained by admitting partial closure of the crack (i.e., closure over specific segments of the crack lips) without overlapping. In this context, they demanded fulfilment of the condition  $K_I=0$  at the crack tip, at which overlapping is expected, imposing, thus, an increasing trend to the  $K_I$  SIF of the opposite crack-tip. Some years later, Dundurs and Comninou [12] proved that, for specific combinations of force and bending moment, applied at infinity, contact between the crack lips cannot be avoided and they provided series of such critical combinations.



The issue of overlapping was thoroughly studied, also, by Theocaris et al. [13], who provided closed-form analytical solutions for the displacements of the lips of a crack in an infinite plate loaded biaxially at infinity. Closed-form expressions for the deformed shape of the crack were given and the limits of validity of the elastic theory were examined, in connection to the overlapping phenomenon. Along the same lines, Pazis et al. [14] concluded that the phenomenon of overlapping “... defines cases where the basic concept of LEFM, that is the complex SIF, which ... characterizes the singular stress field, should be reconsidered”. Moreover, they indicated that “...all mode-II loaded internal cracks present ... overlapping flanks and therefore they belong to physically unacceptable solutions, which should be reconsidered”. Theocaris and Sakellariou [15] arrived at similar conclusions in their attempt to explore whether it is possible or not to implement pure mode-II loading schemes.

The issue of closing crack lips and the associated one of the contact stresses developed are still under intensive study. Solutions for the effective SIF for partially closed ‘mathematical’ cracks under bending were introduced by Beghini and Bertini [16]. They suggested that a LEFM approach ignoring the contact of the crack lips is not acceptable. Some fifteen years ago, Corrado et al. [17] and Carpinteri et al. [18] introduced the ‘overlapping crack model’, while attempting to describe the mechanical response of cracked concrete beams. The model introduced describes according to a satisfactory manner, among others, the size effect, namely the dependence of strength on the size of the specimens. From a completely different starting point (i.e., while seeking solutions for the problem of contact for an arc crack in terms of hypersingular integral equations), Chen et al. [19], arrived at the conclusion that ignoring “...the contact effect for a contact arc crack, the obtained solution for the SIFs is of no sense”. Nowadays, the above mentioned issues are usually (if not exclusively) studied by means of proper numerical schemes, which are based mainly on the Finite- and the Boundary-Element methods [20-25]. On the contrary, purely analytical solutions are relatively scarce in the respective literature [26].

In the light of the above-mentioned discussion, it can be safely concluded that the problem of overlapping crack lips is not as yet closed, although it is definitely indicated by many researchers that, in case it is ignored quite erroneous results are obtained, concerning both the stress field and, also, the values of the respective SIFs. In this direction, a mechanism for properly addressing the overlapping issue is analysed in the next sections of this paper, providing, in addition, closed-form analytical solutions for the stress and displacement fields developed both in the vicinity of the crack tips and, also, along the lips of the crack (contact stresses), as well as naturally sound values for the respective SIFs.

### THE UNNATURAL OVERLAPPING OF THE LIPS OF A ‘MATHEMATICAL’ CRACK IN AN INFINITE PLATE AND THE ASSOCIATED PROBLEM OF NEGATIVE MODE-I SIF

#### *Muskhelishvili’s solution for the first fundamental problem for the infinite cracked plate*

The solution of the first fundamental problem for a ‘mathematical’ crack in an infinite plate was given by Muskhelishvili [27] either by considering the crack as a particular case of an elliptic hole (the minor axis of which tends to zero, becoming, thus, a Griffith-crack) or by addressing the problem as one of linear relationship. For the latter case and using the auxiliary, sectionally holomorphic, function  $\Omega(z)$ , the solution in the  $z=x+iy$  complex plane reads as:

$$\Phi(z) = \frac{(2\Gamma + \bar{\Gamma}')z}{2\sqrt{z^2 - \alpha^2}} - \frac{1}{2}\bar{\Gamma}', \quad \Omega(z) = \frac{(2\Gamma + \bar{\Gamma}')z}{2\sqrt{z^2 - \alpha^2}} + \frac{1}{2}\bar{\Gamma}' \quad (1)$$

For zero rotation at infinity it holds that:

$$\Gamma = \frac{1}{4}(N_1 + N_2), \quad \Gamma' = \frac{1}{4}(N_1 - N_2)e^{-2i\beta} \quad (2, 3)$$

In Eqns.(2,3)  $N_1$  and  $N_2$  are the principal stresses at infinity, and  $\beta$  is the angle between the direction of  $N_1$  and the crack axis. The overbar denotes the conjugate complex value. This solution holds for a coordinate system with  $x$ -axis oriented along the crack and origin located at the mid-point of the crack. It is mentioned here that while obtaining Eqns.(1) the basic assumption of completely stress-free crack lips is adopted. The components of the stress and displacement fields are then expressed in terms of  $\Phi(z)$ ,  $\Omega(z)$  and, also, of  $\varphi(z) = \int \Phi(z)dz$  and  $\omega(z) = \int \Omega(z)dz$  as:

$$\sigma_{xx} + \sigma_{yy} = 4\Re\Phi(z) \quad (4)$$

$$\sigma_{yy} - i\tau_{xy} = \Phi(z) + \Omega(\bar{z}) + (z - \bar{z})\overline{\Phi'(z)} \quad (5)$$

$$2\mu(u + iv) = \kappa\varphi(z) - \omega(\bar{z}) - (z - \bar{z})\overline{\Phi(z)} \quad (6)$$

where prime in Eqn.(5) denotes the derivative with respect to  $z$ , and  $\mu$  is the second Lamé constant (equal to the shear modulus  $G$  of the material of the plate). Moreover,  $\kappa$  is Muskhelishvili's constant, equal to either  $(3-4\nu)$  for plane strain or to  $(3-\nu)/(1+\nu)$  for generalized plane stress conditions, with  $\nu$  denoting Poisson's ratio.

*The 'initial problem' of the cracked plate biaxially loaded at infinity with unnaturally overlapping crack lips*

Some years ago Theocaris et al. [13] and Pazis et al. [14], studied exhaustively the problem of a cracked plate loaded at infinity by the principal stresses  $N_1=\sigma_\infty$  and  $N_2=k\sigma_\infty$  (where  $k$  is the biaxiality ratio, i.e.,  $k=N_2/N_1$ ) (Fig.1), taking advantage of Muskhelishvili's general solution, outlined in previous section.

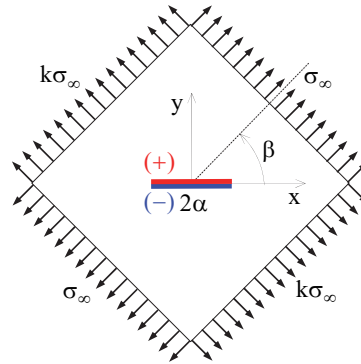


Figure 1: The pre-cracked infinite plate biaxially loaded at infinity.

For the specific configuration, the complex potentials read as follows:

$$\left. \begin{matrix} \Phi_1(z) \\ \Omega_1(z) \end{matrix} \right\} = \frac{\sigma_\infty [(1 - e^{2i\beta}) + k(1 + e^{2i\beta})]z}{4\sqrt{z^2 - \alpha^2}} \pm \frac{\sigma_\infty(1-k)e^{2i\beta}}{4} \quad (7)$$

$$\left. \begin{matrix} \varphi_1(z) \\ \omega_1(z) \end{matrix} \right\} = \frac{\sigma_\infty [(1 - e^{2i\beta}) + k(1 + e^{2i\beta})]\sqrt{z^2 - \alpha^2}}{4} \pm \frac{\sigma_\infty(1-k)e^{2i\beta}z}{4} \quad (8)$$

The motive of Theocaris et al. [13] and Pazis et al. [14] was to describe analytically the shape of the deformed crack, which turned out to be an ellipse. They proved that each one of the two displacement components of any point on the crack lips consists of two distinct terms, i.e., a linear one ( $u_{1, in}^\pm, v_{1, in}^\pm$ ) and an elliptic one ( $u_{1, e}^\pm, v_{1, e}^\pm$ ), reading, respectively, as:

$$\begin{aligned} u_{1, in}^\pm(x) &= c(1-k)\cos 2\beta \cdot x \pm c(1-k)\sin 2\beta \cdot \sqrt{\alpha^2 - x^2} \\ u_{1, e}^\pm & \\ v_{1, in}^\pm(x) &= c(1-k)\sin 2\beta \cdot x \pm c[1+k - (1-k)\cos 2\beta] \cdot \sqrt{\alpha^2 - x^2} \\ v_{1, e}^\pm & \end{aligned} \quad (9)$$

Concerning the parameter  $c$  it holds that:

$$c = \frac{(1+\kappa)\sigma_\infty}{8\mu} \quad (\sigma_\infty > 0) \quad (10)$$

The plus and minus signs in Eqns.(9) denote the upper (red color) and lower (blue color) lip of the crack, respectively, as it is shown in Fig.1. It was proven that, due to the linear terms ( $u_{1, in}^\pm, v_{1, in}^\pm$ ) of the displacement components (which are equal by pairs) the facing points on the crack lips are displaced according to an identical manner (namely as a single point). The respective displacement vector  $u_{1, in}^+(u_{1, in}^+, v_{1, in}^+) = u_{1, in}^-(u_{1, in}^-, v_{1, in}^-) = u_{1, in}$  has constant direction while its magni-



tude varies linearly along the crack, becoming zero at the origin of the reference system (mid-point of the crack). Therefore, these terms are responsible for: (i) a rigid body rotation  $\lambda$ , and (ii) a change of the length of the crack, leading to an intermediate deformed position of the crack, denoted as ‘false-crack’ [13, 14] (Fig.2).

Then, applying the elliptic terms ( $u_{1,e}^{\pm}$ ,  $v_{1,e}^{\pm}$ ) of the displacement components to the facing points of the ‘false-crack’, one obtains the final shape of the deformed crack, which (as already mentioned) is always an ellipse, either open or overlapped. The ‘elliptic’ displacement vector  $v_{1,e}^{\pm}$  ( $u_{1,e}^{\pm}$ ,  $v_{1,e}^{\pm}$ ) forms a constant angle  $\omega$  with respect to the y-axis of the reference system. Angles  $\lambda$  and  $\omega$  are given as follows [13, 14]:

$$\tan \lambda = \left| \frac{c(1-k)\sin 2\beta}{1+c(1-k)\cos 2\beta} \right|, \quad \tan \omega = \left| \frac{(1-k)\sin 2\beta}{1+k-(1-k)\cos 2\beta} \right| \quad (11)$$

As an example, the above mechanism of crack deformation is shown in Fig.2, for an infinite plate made of Plexiglas (with Young’s modulus  $E=3.2$  GPa and Poisson’s ratio  $\nu=0.36$ ), weakened by a ‘mathematical’ crack of length  $2\alpha=0.10$  m and loaded biaxially at infinity by a pair of principal stresses ( $\sigma_{\infty}$ ,  $k\sigma_{\infty}$ ). Assigning numerical values equal to  $\sigma_{\infty}=+1$  GPa (not realistic but it provides clarity to the figure) and  $k=0.2$ , an open crack/ellipse is obtained (see Fig.2a). On the contrary, for the pair  $\sigma_{\infty}= -1$  GPa and  $k=0.1$ , the crack lips overlap each other (see Fig.2b). It is critical to note at this point that the original crack tips of the undeformed crack (i.e., points  $\pm\alpha$ ) are no longer the ‘tips’ of the deformed crack/ellipse (either open or overlapped). In other words, points  $\pm\alpha'$  are not the end-points of the major axis of the deformed crack/ellipse.

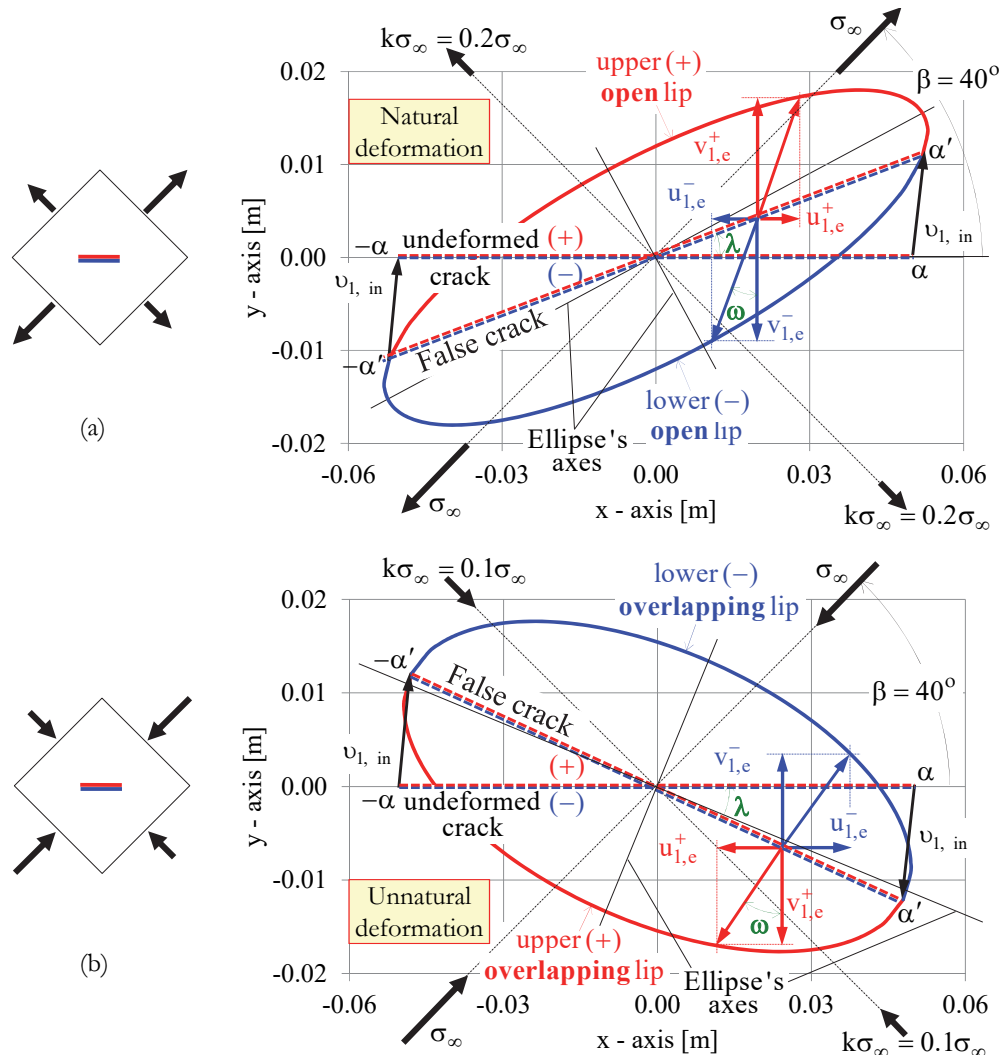


Figure 2: The elliptical shape of the deformed crack for (a) open and (b) overlapping crack lips.

Clearly, crack opening (Fig.2a) is a quite natural phenomenon and for this case the above solution is acceptable, conforming completely to the boundary condition of a crack with stress-free lips. On the contrary, for overlapping crack lips (Fig. 2b), the above solution ceases to be naturally acceptable. In fact, the thickness of the plate prohibits the overlapping of the crack lips and, as a result, contact stresses are generated along the crack lips which cannot be provided by the above presented solution due to the initial assumption of stress-free crack lips. In addition, as it will be discussed in next section, the above described unnatural deformation leads to negative values of the mode-I SIF, undermining definitely the validity of the theoretical analysis of LEFM in the case of closing cracks.

*The unnatural negative stress intensity factor  $K_{I,(1)}$  associated with overlapping lips*

According to the above solution, the mode-I and the mode-II SIFs read as:

$$K_{I,(1)} = \frac{\sigma_\infty \sqrt{\pi\alpha}}{2} [1+k - (1-k)\cos 2\beta], \quad K_{II,(1)} = \frac{\sigma_\infty \sqrt{\pi\alpha}}{2} (1-k)\sin 2\beta \quad (12a, b)$$

Subscript 1 in Eqns.(12) indicates the ‘initial problem’, i.e., the first fundamental problem of the cracked plate (outlined in this section), in which the unnatural overlapping of the crack lips and negative  $K_{I,(1)}$ -values may occur. It is concluded that, in general, when mathematical overlapping is predicted, the mode-I stress intensity factor  $K_{I,(1)}$  becomes negative. Indeed, adopting the numerical values used to draw the overlapping crack lips of Fig.2b (apart from  $\sigma_\infty$ , to which a realistic value equal to  $-1$  MPa is now assigned), the variation of the SIFs (Eqns.(12)) is plotted in Fig.3 versus angle  $\beta$ . It is seen that for the whole range of angles  $\beta$ , for which overlapping occurs ( $0^\circ < \beta < 90^\circ$ ),  $K_{I,(1)}$  is constantly (and unnaturally) negative.

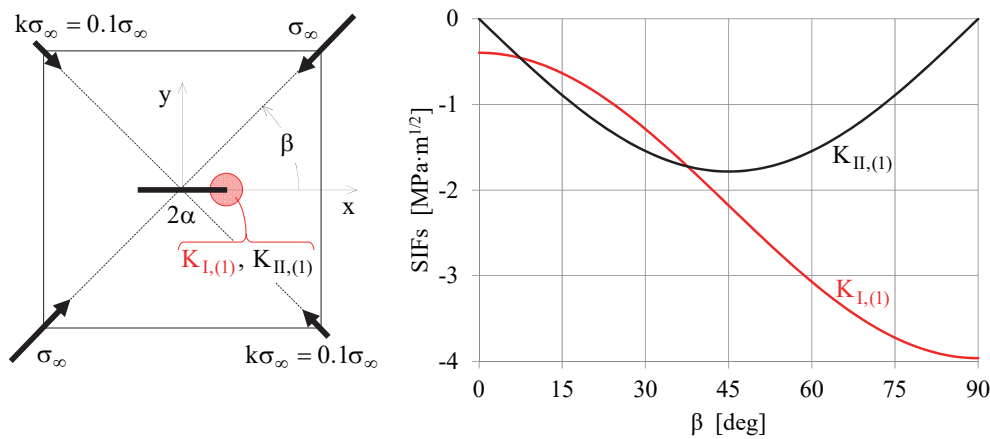


Figure 3: The variation of the SIFs with respect to the angle  $\beta$ .

### ADDRESSING THE OVERLAPPING OF THE CRACK LIPS AND THE NEGATIVE $K_I$ -VALUES IN THE ‘INITIAL PROBLEM’ AND THE RESPECTIVE FIELD OF CONTACT STRESSES

*The mechanism of inverting the overlapping of the crack lips and the nature of the contact stresses*

In this section, an attempt is presented to address the problem of the unnatural overlapping of the crack lips and the closely associated one of the negative  $K_I$ -value in the ‘initial problem’, and, in addition, to provide a solution for the contact stresses, which are inevitably developed along the crack lips. The procedure to confront the specific problem was first outlined in ref.[28]. The underlying idea was that the unnaturally overlapped lips should be “brought back” to a naturally acceptable position, i.e., in mutual contact under the influence of a proper field of contact stresses. In this direction, and considering that overlapping is caused exclusively by the elliptic terms ( $u_{1,e}^\pm, v_{1,e}^\pm$ ) of the displacements (while, on the contrary, the respective linear displacement vector  $v_{1, in}$  is naturally accepted), the problem is addressed by inverting specific portions of the elliptic displacements, namely,  $\tau \cdot u_{1,e}^\pm, \delta \cdot v_{1,e}^\pm$ , where parameters  $\tau$  and  $\delta$  are defined as:

$$0 \leq \tau \leq 1, \quad \delta(\tau) = (1 - \tau) \cdot \tan \lambda \cdot \tan \omega + 1 \quad (13)$$

Retaining the linear terms of the displacement, the naturally acceptable deformed crack is directed along the ‘false crack’. The contact stresses developed between the lips of the crack are analogous to the degree of overlapping, since they are equal to the stresses required to bring back the overlapping lips in their naturally accepted position of mutual contact. The mechanism of inverting the overlapping of the lips and obtaining a naturally acceptable deformed configuration, as well as the contact stresses developed along the crack lips, are graphically shown in Figs.4(a) and 4(b), respectively.

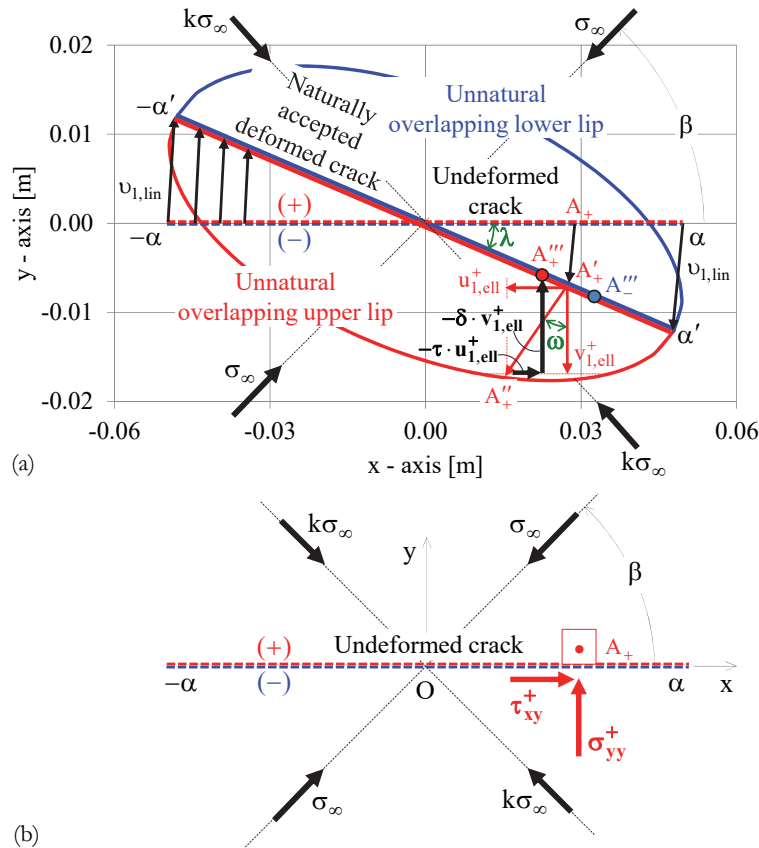


Figure 4: (a) The mechanism of inverting overlapping and obtaining a naturally acceptable deformed crack, and (b) the respective contact stresses exerted by the lower to the upper lip.

More analytically, a point  $A_+$  on the upper lip  $-\alpha\alpha$  of the undeformed crack is considered:

- As a first step, point  $A_+$ , shifts, due to the linear displacement vector  $v_{1,lin}$ , to a point  $A'_+$  on the ‘false crack’.
- In turn, point  $A'_+$  shifts, due to the elliptic displacements,  $(u_{1,e}^+, v_{1,e}^+)$ , to point  $A''_+$  on the overlapping upper lip (red color in Fig.4).
- Then, applying to  $A''_+$  the inverse elliptic displacements  $(-\tau \cdot u_{1,e}^+, -\delta \cdot v_{1,e}^+)$ , point  $A''_+$  shifts further to its final position  $A'''_+$  on the naturally accepted deformed crack  $-\alpha\alpha'$  (which has the direction of the ‘false crack’).

Similarly, point  $A_-$ , on the lower lip of the undeformed crack  $-\alpha\alpha$ , originally facing point  $A_+$ , occupies finally the position  $A'''_-$  on the naturally accepted deformed crack lip  $-\alpha\alpha'$  (the relevant displacements are omitted from Fig.4a for clarity reasons). The above described deformation scheme corresponds to the most general case, i.e., that for which the lips of the crack slide relatively to each other.

The respective normal  $\sigma_{yy}^+$  and frictional  $\tau_{xy}^+$  contact stresses (equal in magnitude to those causing  $-\tau \cdot u_{1,e}^+, -\delta \cdot v_{1,e}^+$ ), acting to  $A_+$  from  $A_-$ , are shown in Fig.4b. Clearly the same stresses are exerted to  $A_-$  from  $A_+$  (which are not drawn in Fig.4b, again for obvious reasons of figure clarity).

From the analytical point of view, the above-described procedure for addressing the overlapping of the crack lips in the ‘initial problem’ is realized by superposing to it an auxiliary mixed fundamental problem, called the ‘inverse problem’ (Fig. 5). The resulting problem is a mixed fundamental problem, called the ‘general problem’, without overlapping.

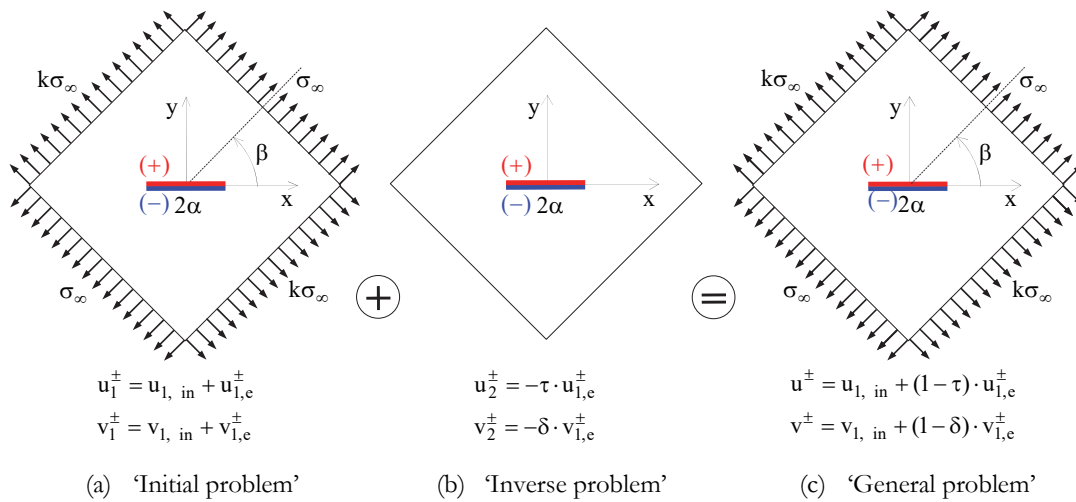


Figure 5: Superposing to the ‘initial problem’ (a) the ‘inverse problem’ (b), and the resulting physically acceptable ‘general problem’ (c).

The ‘general problem’ provides physically acceptable solutions for stresses, displacements and SIFs, either in case of an open crack or of a crack at impending overlapping in the ‘initial problem’. Subscript 2 is used in the formulae of the ‘inverse problem’ to distinguish from the ‘initial problem’ with subscript 1, while in the ‘general problem’ there is no index. Recapitulating, it can be said that, in case the stresses at infinity lead to an open crack, then  $\tau$  and  $\delta$  should be set zero, and the ‘general problem’ reduces to the ‘initial problem’ (the ‘inverse problem’ disappears), which in this case is naturally acceptable. On the contrary, in case the stresses at infinity lead the ‘initial problem’ to overlapping lips,  $\tau$  and  $\delta$  should take values according to Eqns.(13), leading to an acceptable solution without overlapping, according to the ‘general problem’. Regarding the numerical values of  $\tau$  and  $\delta$ , it is stressed out that Eqns.(13) refer to all possible magnitudes of the relative displacement of the crack lips, dictated by the value of  $\tau$ . However, energy conservation considerations, required to fulfill the validity of Lamé’s constitutive law adopted, restrict investigation in the following two limiting cases:

- i) *Absence of friction between the lips of the crack.* It corresponds to the maximum magnitude of the relative displacement of the crack lips. One lip slides smoothly on the other and the original crack tips  $\pm\alpha$  in the deformed position  $\pm\alpha'$  are no longer the tips of the deformed crack, due to the relative sliding of the crack lips. Then, Eqns.(13) become:

$$\tau = 0, \quad \delta = \delta_{\max} = \tan \lambda \cdot \tan \omega + 1 \tag{14}$$

- ii) *Presence of friction between the lips of the crack.* In this case, in order to avoid energy loss (by heat dissipation), the assumption is made that the friction coefficient between the crack lips prohibits completely relative displacement of the crack lips. Then, due to the absence of any relative sliding between the lips of the crack, points  $\pm\alpha'$  remain the tips of the deformed crack. In this case Eqns.(13) become:

$$\tau = \delta = 1 \tag{15}$$

*The solution of the ‘inverse problem’: A mixed fundamental problem*

The solution of the ‘initial problem’ was shortly outlined in previous section. In this section, the solution of the ‘inverse problem’ (Fig.5b) is, also, outlined for the completeness of the present analysis. The boundary conditions of the ‘inverse problem’ (a mixed fundamental problem) are: (i) zero stresses at infinity, and (ii) opposite portions of the elliptic displacements of the ‘initial problem’ (see Eqns.(9), (10)) on the crack lips, namely:

$$\begin{aligned} u_2^\pm = -\tau \cdot u_{1,e}^\pm &= \tau \cdot \frac{(1 + \kappa)\sigma_\infty}{8\mu} (1 - k) \sin 2\beta \cdot \sqrt{\alpha^2 - x^2} \\ v_2^\pm = -\delta \cdot v_{1,e}^\pm &= \delta \cdot \frac{(1 + \kappa)\sigma_\infty}{8\mu} [1 + k - (1 - k) \cos 2\beta] \cdot \sqrt{\alpha^2 - x^2} \end{aligned} \tag{16}$$

Following Muskhelishvili [27], the problem is here solved as a problem of linear relationship. In this context, Eqn.(6) yields for the displacements of the upper (+) and lower (-) crack lips, respectively, the following relations:



$$2\mu(u_2^+ + iv_2^+) = \kappa\varphi_2^+(x) - \omega_2^-(x) \tag{17}$$

$$2\mu(u_2^- + iv_2^-) = \kappa\varphi_2^-(x) - \omega_2^+(x) \tag{18}$$

By adding Eqns.(17) and (18) it is obtained:

$$\left[ \frac{\kappa\varphi_2(x) - \omega_2(x)}{X_o(x)} \right]^+ - \left[ \frac{\kappa\varphi_2(x) - \omega_2(x)}{X_o(x)} \right]^- = 0 \tag{19}$$

where

$$X_o^\pm(x) = \frac{1}{\pm i\sqrt{\alpha^2 - x^2}} \tag{20}$$

are values attained by the sectionally holomorphic function:

$$X_o(z) = \frac{1}{\sqrt{z^2 - \alpha^2}} \tag{21}$$

when  $z$  approaches  $x$  on the upper (+) and lower (-) crack lips, respectively. From Eqn.(19) it is deduced that the function  $[\kappa\varphi_2(z) - \omega_2(z)]/X_o(z)$  is holomorphic (single-valued) on the crack and, in turn, everywhere on  $z$ -plane. Since  $X_o(z)$  is double-valued on the crack, it is deduced that  $\kappa\varphi_2(z) - \omega_2(z)$  must be zero there and, in turn, on the entire  $z$ -plane. Therefore:

$$\omega_2(z) = \kappa\varphi_2(z) \tag{22}$$

Now, subtracting Eqn.(17) from Eqn.(18), and using, in addition, Eqns.(22) and (16), one obtains that:

$$\varphi_2^+(x) - \varphi_2^-(x) = -\frac{(1 + \kappa)\sigma_\infty}{4\kappa} \left\{ \tau \cdot (1 - k) \sin 2\beta \cdot \sqrt{\alpha^2 - x^2} + i\delta [1 + k - (1 - k) \cos 2\beta] \cdot \sqrt{\alpha^2 - x^2} \right\} \tag{23}$$

For large  $|z|$ ,  $\varphi_2(z)$  reads as [27]:

$$\varphi_2(z) = -\frac{X + iY}{2\pi(\kappa + 1)} \text{og}z + \Gamma_2 z + \varphi_{2,o}(z) \tag{24}$$

where  $(X, Y)$  is the resultant vector of external forces acting on the crack (for the problem studied here it is zero),  $\Gamma_2$  is zero according to Eqn.(2) and the boundary conditions at infinity, and  $\varphi_{2,o}(z)$  is a function holomorphic on the entire plane. Thus, for large  $|z|$ , it holds that  $\varphi_2(z) = \varphi_{2,o}(z)$ . Taking into account that the displacement (Eqn.(6)) must be zero at infinity, it should hold that  $\varphi_{2,o}(z) = 0$  at infinity and, thus,  $\varphi_2(z \rightarrow \infty) = 0$ . In this context, the solution of Eqn.(23) for  $\varphi_2(z)$  becomes:

$$\varphi_2(z) = \frac{-1}{2\pi i} \int_{-\alpha}^{+\alpha} \frac{(1 + \kappa)\sigma_\infty}{4\kappa} \left\{ \tau \cdot (1 - k) \sin 2\beta \cdot \sqrt{\alpha^2 - x^2} + i\delta [1 + k - (1 - k) \cos 2\beta] \cdot \sqrt{\alpha^2 - x^2} \right\} \frac{dx}{x - z} \tag{25}$$

Taking advantage of familiar properties of the Cauchy-type integrals it can be written that:

$$\varphi_2(z) = -\frac{(1 + \kappa)\sigma_\infty}{8\kappa} \left\{ \delta \cdot [1 + k - (1 - k) \cos 2\beta] - i \cdot \tau \cdot (1 - k) \sin 2\beta \right\} \cdot \left( \sqrt{z^2 - \alpha^2} - z \right) \tag{26}$$

Combination of Eqns.(26) and (22) yields:

$$\omega_2(z) = -\frac{(1 + \kappa)\sigma_\infty}{8} \left\{ \delta \cdot [1 + k - (1 - k) \cos 2\beta] - i \cdot \tau \cdot (1 - k) \sin 2\beta \right\} \cdot \left( \sqrt{z^2 - \alpha^2} - z \right) \tag{27}$$



Upon differentiation of the expressions of Eqn.(26) and (27) it is obtained that:

$$\Phi_2(z) = -\frac{(1+\kappa)\sigma_\infty}{8\kappa} \left\{ \delta \cdot [1+k - (1-k)\cos 2\beta] - i \cdot \tau \cdot (1-k)\sin 2\beta \right\} \cdot \left( \frac{z}{\sqrt{z^2 - \alpha^2}} - 1 \right) \quad (28)$$

$$\Omega_2(z) = -\frac{(1+\kappa)\sigma_\infty}{8} \left\{ \delta \cdot [1+k - (1-k)\cos 2\beta] - i \cdot \tau \cdot (1-k)\sin 2\beta \right\} \cdot \left( \frac{z}{\sqrt{z^2 - \alpha^2}} - 1 \right) \quad (29)$$

Substituting in Eqn.(5) from Eqns.(28) and (29), and letting  $z$  tend to  $x$  on the upper and lower crack lips, the stresses on the crack lips due to the ‘inverse problem’ read as:

$$\sigma_{yy,2}^\pm = \frac{(1+\kappa)^2\sigma_\infty}{8\kappa} \delta \cdot [1+k - (1-k)\cos 2\beta] \pm \frac{(1-\kappa^2)\sigma_\infty}{8\kappa} \tau \cdot (1-k)\sin 2\beta \frac{x}{\sqrt{\alpha^2 - x^2}} \quad (30)$$

$$\tau_{xy,2}^\pm = \frac{(1+\kappa)^2\sigma_\infty}{8\kappa} \tau \cdot (1-k)\sin 2\beta \mp \frac{(1-\kappa^2)\sigma_\infty}{8\kappa} \delta \cdot [1+k - (1-k)\cos 2\beta] \frac{x}{\sqrt{\alpha^2 - x^2}} \quad (31)$$

The stresses provided by Eqns.(30) and (31) correspond to the inversion of overlapping and could stand for the contact stresses developed on the crack lips, prohibiting overlapping. However, as it will be proven in next section, only specific portions of the above determined stresses may be considered as contact stresses.

*The contact stresses on the lips of the crack*

To clarify the last point raised in previous section, and in order to obtain the contact stresses developed on the crack lips, consider the problem of the infinite cracked plate under uniaxial compression normal to the crack (i.e.,  $-\sigma_\infty$ ,  $k=0$ ,  $\beta=90^\circ$ ), which produces the unacceptable overlapping crack-ellipse  $L$  (Fig.6a). In this case, the ‘inverse problem’ of Fig.6b should be superimposed to the ‘initial problem’ of Fig.6. Namely, since there is no relative displacement of the crack lips along the  $x$ -direction in the ‘initial problem’,  $\tau$  should be set, according to the present approach, equal to zero, while  $\delta$  should be set equal to unity. In this case the boundary displacements on the crack in the ‘inverse problem’ read as:  $u_2^\pm = 0$ ,  $v_2^\pm = -1 \cdot v_{1,e}^\pm$  (Fig.6b).

Clearly, such boundary displacements on the crack do not permit Poisson’s shrinkage along  $x$ -direction, something achieved by the generation of tangential stresses on the crack in the ‘inverse problem’, reading (according to Eqn.(31)) as:

$$\tau_{xy,p}^\pm = \frac{(1-\kappa^2)\sigma_\infty}{8\kappa} \delta \cdot [1+k - (1-k)\cos 2\beta] \frac{x}{\sqrt{\alpha^2 - x^2}}, \quad (\text{with } \delta = 1, k = 0, \beta = 90^\circ) \quad (32)$$

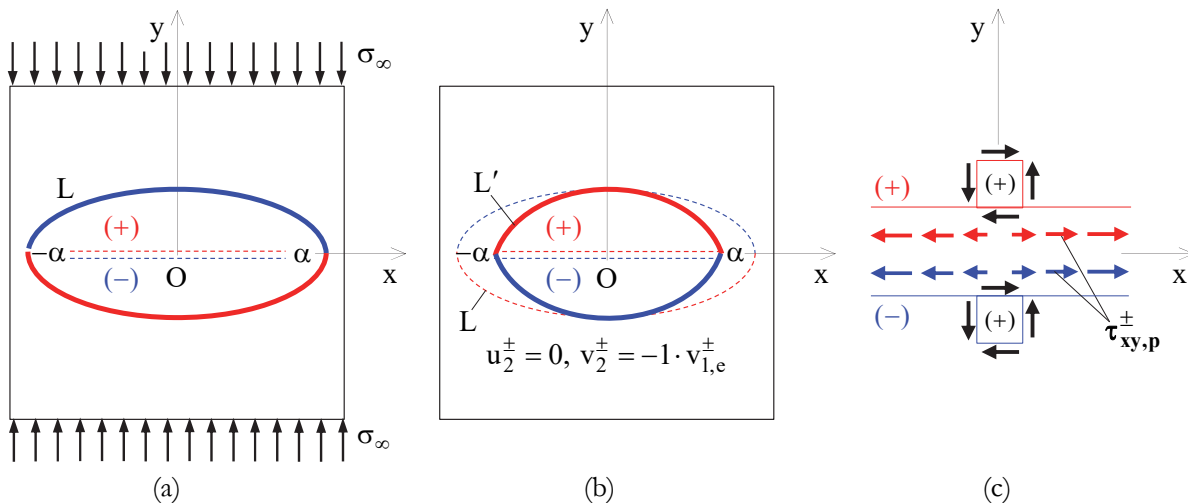


Figure 6: (a) The unacceptable overlapping, (b) the boundary displacements imposed to the crack lips in the ‘inverse problem’ preventing overlapping, (c) the ‘parasitic’ tangential stresses.



The tangential stresses given by Eqn.(32) are zeroed at the midpoint of the crack, and have the same outwards direction on both lips (towards the crack tips (see Fig.6c)), where they become unbounded. These stresses are necessary in order to keep the crack lips stationary along the x-direction, prohibiting the aforementioned Poisson's effect.

This kind of stresses, denoted hereafter as 'parasitic' (indicated by the subscript 'p' in Eqn.(32)), cannot be considered as contact stresses (the reason for their generation may be attributed to the fact that the linear terms of the displacement vector were accepted as they are provided by the traditional LEFM solution of the 'initial problem'). Therefore, they should be subtracted from Eqn.(31) which reduces to:

$$\tau_{xy}^{\pm} = \frac{(1+\kappa)^2 \sigma_{\infty}}{8\kappa} \tau \cdot (1-k) \sin 2\beta \tag{33}$$

Similarly, it is found that:

$$\sigma_{yy}^{\pm} = \frac{(1+\kappa)^2 \sigma_{\infty}}{8\kappa} \delta \cdot [1+k - (1-k) \cos 2\beta] \tag{34}$$

Eqns.(33) and (34) provide, respectively, the frictional (shear) and the compressive (normal) contact stresses, which are developed along the lips of the crack in case it is at a state of impending overlapping. In Eqns.(33) and (34) the subscript 2 has been omitted, since stresses calculated on the crack lips by the 'inverse' and the 'general problem' are identical to each other (because in the 'initial problem' the crack is free from stresses). As it is obvious, the contact stresses developed are uniformly distributed along the crack.

*The Stress Intensity Factors (SIFs) in the 'inverse problem'*

In order now to calculate the Stress Intensity Factors (SIFs) in the 'inverse problem', one should substitute in Eqn.(5) the expressions from Eqns.(28) and (29). Then letting z tend to x out of the crack, the stresses in the plate along x-axis due to the 'inverse problem' are written as:

$$\sigma_{yy,2} = -\frac{(1+\kappa)^2 \sigma_{\infty}}{8\kappa} \delta \cdot [1+k - (1-k) \cos 2\beta] \left( \frac{x}{\sqrt{x^2 - \alpha^2}} - 1 \right) \tag{35}$$

$$\tau_{xy,2} = -\frac{(1+\kappa)^2 \sigma_{\infty}}{8\kappa} \tau \cdot (1-k) \sin 2\beta \left( \frac{x}{\sqrt{x^2 - \alpha^2}} - 1 \right) \tag{36}$$

Then the mode-I and mode-II SIFs in the 'inverse problem' become:

$$K_{I,(2)} = \sqrt{2\pi} \lim_{z \rightarrow \alpha} [\sigma_{yy,2} \sqrt{z - \alpha}] = -\frac{(1+\kappa)^2 \sigma_{\infty} \sqrt{\pi\alpha}}{8\kappa} \delta \cdot [1+k - (1-k) \cos 2\beta] \tag{37}$$

$$K_{II,(2)} = \sqrt{2\pi} \lim_{z \rightarrow \alpha} [\tau_{xy,2} \sqrt{z - \alpha}] = -\frac{(1+\kappa)^2 \sigma_{\infty} \sqrt{\pi\alpha}}{8\kappa} \tau \cdot (1-k) \sin 2\beta \tag{38}$$

*The final, naturally accepted 'general problem'*

Superposing Eqns.(7) and (8) to Eqns.(26-29), the solution of the 'general problem' is obtained as:

$$\varphi(z) = \frac{\sigma_{\infty}}{4} \left\{ [1+k - (1-k)e^{2i\beta}] \sqrt{z^2 - \alpha^2} + (1-k)e^{2i\beta} z \right\} - \frac{(1+\kappa)\sigma_{\infty}}{8\kappa} \left\{ \delta \cdot [1+k - (1-k) \cos 2\beta] - i \cdot \tau \cdot (1-k) \sin 2\beta \right\} \cdot \left( \sqrt{z^2 - \alpha^2} - z \right) \tag{39}$$

$$\omega(z) = \frac{\sigma_{\infty}}{4} \left\{ [1+k - (1-k)e^{2i\beta}] \sqrt{z^2 - \alpha^2} - (1-k)e^{2i\beta} z \right\} - \frac{(1+\kappa)\sigma_{\infty}}{8\kappa} \left\{ \delta \cdot [1+k - (1-k) \cos 2\beta] - i \cdot \tau \cdot (1-k) \sin 2\beta \right\} \cdot \left( \sqrt{z^2 - \alpha^2} - z \right) \tag{40}$$



$$\Phi(z) = \frac{\sigma_\infty}{4} \left\{ \left[ 1+k-(1-k)e^{2i\beta} \right] \frac{z}{\sqrt{z^2-\alpha^2}} + (1-k)e^{2i\beta} \right\} - \frac{(1+\nu)\sigma_\infty}{8\nu} \left\{ \delta \cdot [1+k-(1-k)\cos 2\beta] - i \cdot \tau \cdot (1-k)\sin 2\beta \right\} \cdot \left( \frac{z}{\sqrt{z^2-\alpha^2}} - 1 \right) \tag{41}$$

$$\Omega(z) = \frac{\sigma_\infty}{4} \left\{ \left[ 1+k-(1-k)e^{2i\beta} \right] \frac{z}{\sqrt{z^2-\alpha^2}} - (1-k)e^{2i\beta} \right\} - \frac{(1+\nu)\sigma_\infty}{8} \left\{ \delta \cdot [1+k-(1-k)\cos 2\beta] - i \cdot \tau \cdot (1-k)\sin 2\beta \right\} \cdot \left( \frac{z}{\sqrt{z^2-\alpha^2}} - 1 \right) \tag{42}$$

In particular, the displacements of the crack lips are obtained (by adding Eqns.(9) and (16)) as:

$$u^\pm(x) = u_1^\pm + u_2^\pm = \frac{(1+\nu)\sigma_\infty}{8\mu} \left\{ (1-k)\cos 2\beta \cdot x \pm (1-\tau)(1-k)\sin 2\beta \cdot \sqrt{\alpha^2-x^2} \right\}$$

$$v_1^\pm(x) = v_1^\pm + v_2^\pm = \frac{(1+\nu)\sigma_\infty}{8\mu} \left\{ (1-k)\sin 2\beta \cdot x \pm (1-\delta)[1+k-(1-k)\cos 2\beta] \cdot \sqrt{\alpha^2-x^2} \right\} \tag{43}$$

and the respective contact stresses on the crack lips in the ‘general problem’ are given by Eqns.(33) and (34). Regarding the SIFs in the ‘general problem’, they are obtained by superposing Eqns.(12) to Eqns.(37) and (38), and they are written as:

$$K_I = \frac{\sigma_\infty \sqrt{\pi\alpha}}{2} \left[ 1 - \frac{(1+\nu)^2}{4\nu} \delta \right] [1+k-(1-k)\cos 2\beta]$$

$$K_{II} = \frac{\sigma_\infty \sqrt{\pi\alpha}}{2} \left[ 1 - \frac{(1+\nu)^2}{4\nu} \tau \right] (1-k)\sin 2\beta \tag{44}$$

Eqns.(44) should hold for any  $\tau$  and  $\delta$  values, including the limiting case  $\tau=\delta=1$  of Eqn.(15). But in this case, since any relative displacement between the crack lips is prohibited, it holds that  $K_I=K_{II}=0$ , which (from Eqns.(44)) provides:

$$1 - \frac{(1+\nu)^2}{4\nu} = 0 \tag{45}$$

Eqn.(45) is only satisfied if the plate is under plane strain ( $\nu=3-4\nu$ ) and, in addition, the Poisson’s ratio is equal to  $\nu=0.5$  (i.e., if the material has exceeded the yield point). Thus, under the linear elastic assumption adopted here, Eqn.(45) cannot be satisfied. In this context, and in order to fulfill the condition  $K_I=K_{II}=0$  for  $\tau=\delta=1$ , the SIFs in the ‘inverse problem’ (Eqns.(37) and (38)) must be redefined as follows:

$$K'_{I,(2)} = \frac{4\nu}{(1+\nu)^2} K_{I,(2)} = -\frac{\sigma_\infty \sqrt{\pi\alpha}}{2} \delta \cdot [1+k-(1-k)\cos 2\beta]$$

$$K'_{II,(2)} = \frac{4\nu}{(1+\nu)^2} K_{II,(2)} = -\frac{\sigma_\infty \sqrt{\pi\alpha}}{2} \tau \cdot (1-k)\sin 2\beta \tag{46}$$

which upon superposition to Eqns.(12) yield the final naturally acceptable expressions:

$$K_I = \frac{\sigma_\infty \sqrt{\pi\alpha}}{2} (1-\delta)[1+k-(1-k)\cos 2\beta] \tag{47}$$

$$K_{II} = \frac{\sigma_\infty \sqrt{\pi\alpha}}{2} (1-\tau)(1-k)\sin 2\beta \tag{48}$$

**THE CRACKED VERSUS THE INTACT PLATE UNDER UNIAXIAL COMPRESSION**

Based on the formulae obtained in previous section, displacements, stresses and SIFs are here calculated approximately for a uniaxially compressed square plate, with a short central ‘mathematical’ crack  $2\alpha$  (Fig.7a). In this configuration, apart from the limiting case  $\beta=0^\circ$ , the ‘initial problem’ provides always unnatural overlapping lips, while the ‘general problem’ introduced in this paper provides always closed cracks with lips under mutual contact stresses. In addition, the intact plate under an identical loading scheme (Fig. 7b) is studied in parallel with the cracked plate in an attempt to quantify the actual consequences of the presence of the crack on the displacement and stress fields.

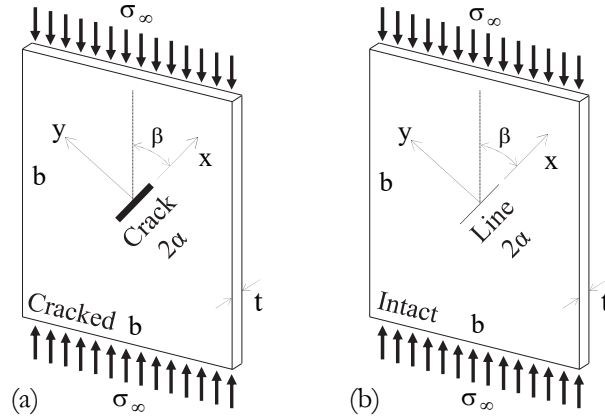


Figure 7: (a) The cracked plate uniaxially compressed, and (b) the relevant intact plate under the same loading conditions.

*The intact plate under uniaxial compression*

The complex potentials solving the infinite intact plate under uniaxial pressure, for the xOy system shown in Fig.7b, are:

$$\varphi_{in}(z) = \frac{\sigma_\infty}{4}z, \quad \psi_{in}(z) = -\frac{\sigma_\infty}{2}e^{-2i\beta}z, \quad \Phi_{in}(z) = \frac{\sigma_\infty}{4}, \quad \Psi_{in}(z) = -\frac{\sigma_\infty}{2}e^{-2i\beta} \tag{49}$$

Substituting from Eqns.(49) in the well-known formulae [27]:

$$\sigma_{xx,in} + \sigma_{yy,in} = 4\Re\Phi_{in}(z), \quad \sigma_{yy,in} - i\tau_{xy,in} = 2\Re\Phi_{in}(z) + z\overline{\Phi'_{in}(z)} + \overline{\Psi_{in}(z)} \tag{50}$$

$$2\mu(u_{in} + iv_{in}) = \kappa\varphi_{in}(z) - z\overline{\Phi_{in}(z)} - \overline{\psi_{in}(z)} \tag{51}$$

stresses and displacements in the plate are obtained as:

$$\sigma_{xx,in} = \frac{\sigma_\infty}{2}(1 + \cos 2\beta), \quad \sigma_{yy,in} = \frac{\sigma_\infty}{2}(1 - \cos 2\beta), \quad \tau_{xy,in} = \frac{\sigma_\infty}{2}\sin 2\beta \tag{52}$$

$$u_{in} = \frac{\sigma_\infty}{4\mu} \left( \frac{\kappa-1}{2}x + x \cos 2\beta + y \sin 2\beta \right), \quad v_{in} = \frac{\sigma_\infty}{4\mu} \left( \frac{\kappa-1}{2}y - y \cos 2\beta + x \sin 2\beta \right) \tag{53}$$

*Comparing the displacement field for a cracked plate versus that for an intact plate*

The deformed shapes of an intact and a cracked plate, for both unnaturally overlapping lips (of only theoretical interest) and naturally acceptable lips in contact, are obtained in this section. In this context, two square plates ABCD, an intact and a cracked one, of side-length  $b=0.40$  m, are compressed by uniform pressure  $\sigma_\infty$  on their sides AB and CD. In the cracked plate, the crack length is  $2\alpha=0.10$  m and forms an angle  $\beta=30^\circ$  with  $\sigma_\infty$ . The material of both plates is PMMA with  $E=3.2$  GPa and  $\nu=0.36$ . For clarity of the figures, an extremely large  $\sigma_\infty$  ( $-1$  GPa) is assumed. To draw the deformed configuration of the intact plate use is made of Eqns.(53). In drawing the deformed configuration of the cracked plate for the unnatural overlapping, use is made of Eqns.(6-9) of the unnatural ‘initial problem’, for  $k=0$ . The two deformed configurations are shown in juxtaposition to each other in Fig.8, for plane strain conditions; black color is used for the cracked plate and red color is used for the intact one. The undeformed plate ABCD is also shown with black discontinuous line.

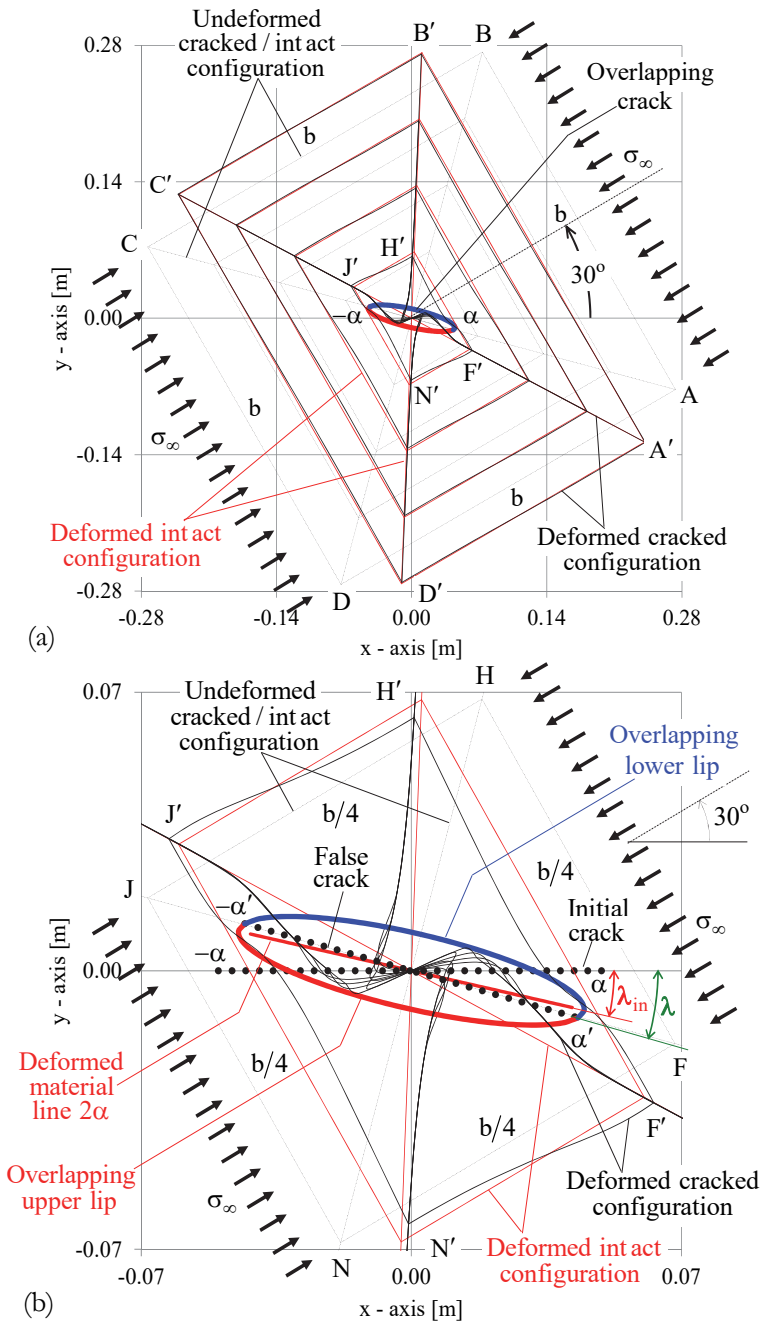


Figure 8: (a) The deformed versus the undeformed configuration of the intact and the cracked plates in juxtaposition to each other, admitting the unnatural overlapping, and (b) a magnified view of the immediate vicinity of the overlapping crack.

Apart from the square ABCD, three additional confocal squares on the plates' cross-sections, of length 0.3, 0.2, 0.1 m, as well as their diagonals, are shown in Fig.8a, before and after deformation. In addition, the crack is shown before and after deformation, with its overlapping lips marked red for the upper and blue for the lower lip. A magnified view of the immediate vicinity of the overlapping crack is shown in Fig.8b. Namely, the square FHJN of side-length  $b/4=0.1$  m, and the enclosed initial crack  $2\alpha$ , are shown before and after deformation. Clearly, for the cracked plate, the deformed square F'H'J'N' and the diagonals have been strongly distorted, following the deformation of the overlapping lips, contrary to the respective deformed square of the intact plate (red color) that has remained a rectilinear rectangular. What is worth noticing is that, even in the case of the unnatural overlapping, and basically upon the assumption of an extreme high pressure, moving away from the crack, the displacement fields of the cracked and the intact plates seem to converge rapidly. The same example is next repeated adopting the solution of the 'general problem' without overlapping, but with the crack lips fully in contact. The results are shown in Fig.9. To draw the deformed configuration in Fig.9, use was made of Eqns.

(6) and (39-41), for the interior of the cracked plate, and Eqns.(43) for the deformed closed crack without overlapping (the upper lip is marked with red continuous line and the lower one with blue discontinuous line). In all expressions it was set  $k=0$ . In addition, the choice of smooth contact between the lips of the crack was made, in which case the coefficients  $\tau$  and  $\delta$  appearing in Eqns.(39-41) and (43) are given by Eqns.(14) (for maximum relative slip between the lips of the crack).

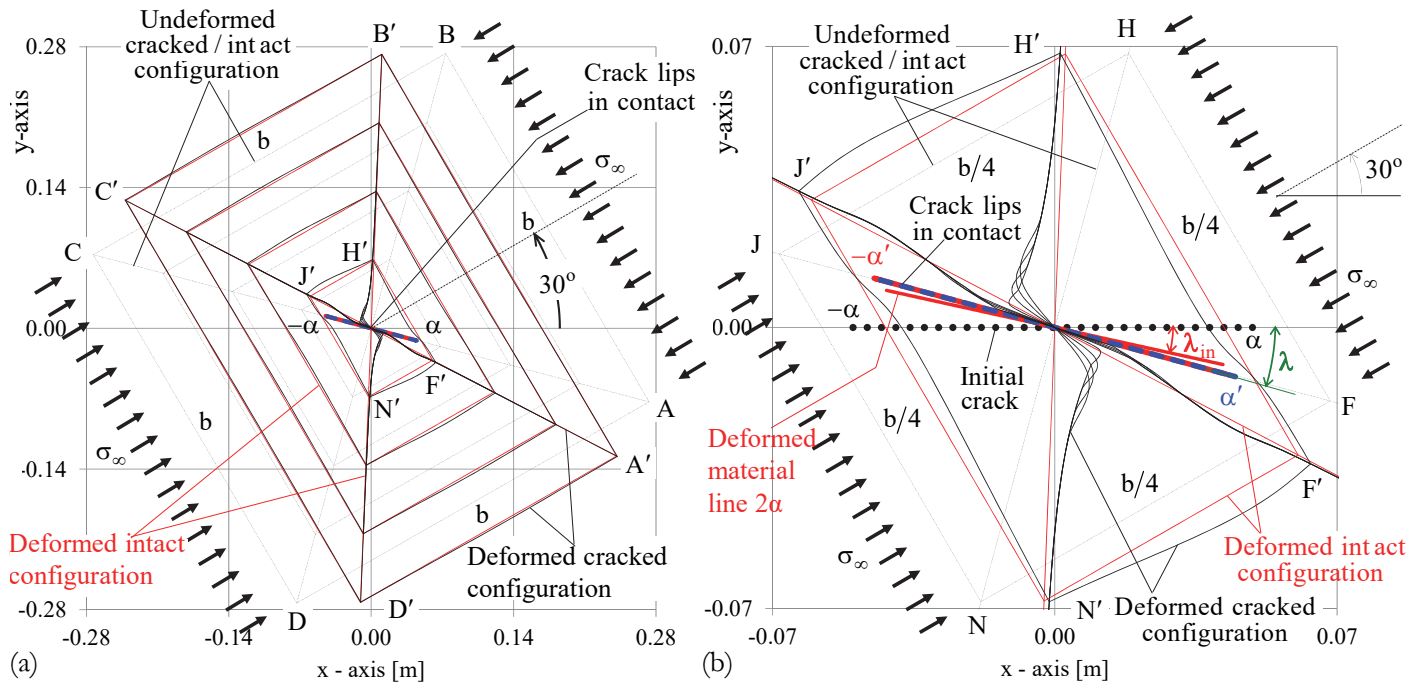


Figure 9: (a) The deformed versus the undeformed configuration of the intact and the cracked plates in juxtaposition, due to the solution of the physically acceptable ‘general problem’, and (b) a magnified view of the immediate vicinity of the closed crack.

From Fig.9 it is again seen that the displacements of the intact and the cracked plate converge rapidly, while moving away from the crack. Of course, while closely approaching the crack, the deformations of the intact and the cracked plates diversify significantly from each other due to the rigid body rotation  $\lambda$  of the crack and the (maximum) relative sliding of its lips. Regarding this issue, a point on the upper crack lip near the initial crack tip  $-\alpha$ , is the new crack tip  $-\alpha'$  on the deformed crack (Fig.9b). Analogously, a point on the lower crack lip near the initial crack tip  $\alpha$ , is the new crack tip  $\alpha'$  on the deformed crack. A clear difference is, also, seen between the unnatural overlapping and the natural closed crack cases. For the overlapping case the corners H', N' shrink towards the center of the crack due to the overlapping (Fig.8b), while for the naturally acceptable closed crack, points on lines H'J', N'F', move away from the crack because of its rotation (Fig. 9b). Finally, note that angle  $\lambda$  of the ‘false crack’ (Eqns.(11) for  $k=0$ ) in Fig.2, and the rigid body rotation  $\lambda$  of the crack in Fig.9b, are identical (since the linear terms of displacements were accepted as provided by the original LEFM solution). However,  $\lambda$  exceeds the rigid body rotation  $\lambda_{in}$  of the line segment  $2\alpha$  of the intact disc (as calculated from Eqns.(53):

$$\lambda_{in} = \tan^{-1} \left| \frac{2 \sin 2\beta}{(\kappa - 1 + 2 \cos 2\beta) \sigma_\infty + 8\mu} \sigma_\infty \right| < \lambda = \tan^{-1} \left| \frac{(1 + \kappa) \sin 2\beta}{(1 + \kappa) \cos 2\beta \sigma_\infty + 8\mu} \sigma_\infty \right| \quad (54)$$

(It is to be noted that the direction of  $-\alpha'\alpha'$  does not coincide with JF direction, as it appears incidentally in Fig.9b).

### Comparing the stress field for a cracked plate versus that for an intact plate

The two plates ABCD made of PMMA, intact and cracked, considered in the previous section, are submitted to uniform pressure  $\sigma_\infty = -1$  MPa along their sides AB and CD. Again, in the cracked plate, the length of the crack is  $2\alpha = 0.10$  m and angle  $\beta = 30^\circ$ . The stress fields are first studied in the interior of the intact and the cracked plate. In this context, the stresses in a system  $x'Oy'$  at  $30^\circ$  with respect to the system  $xOy$  are plotted along the sides BA, CB, and the interior lines HF, JH. In addition, the stresses are plotted along the diagonals OB and OA. In all cases, distinction is made between the cases of absence and presence of friction along the crack lips. In plotting stresses in the cracked plate, use was made of Eqns.(4), (5), (41) and (42), for  $k=0$ , while for the intact plate Eqns.(52) were used. The results are plotted in Figs.10-15.

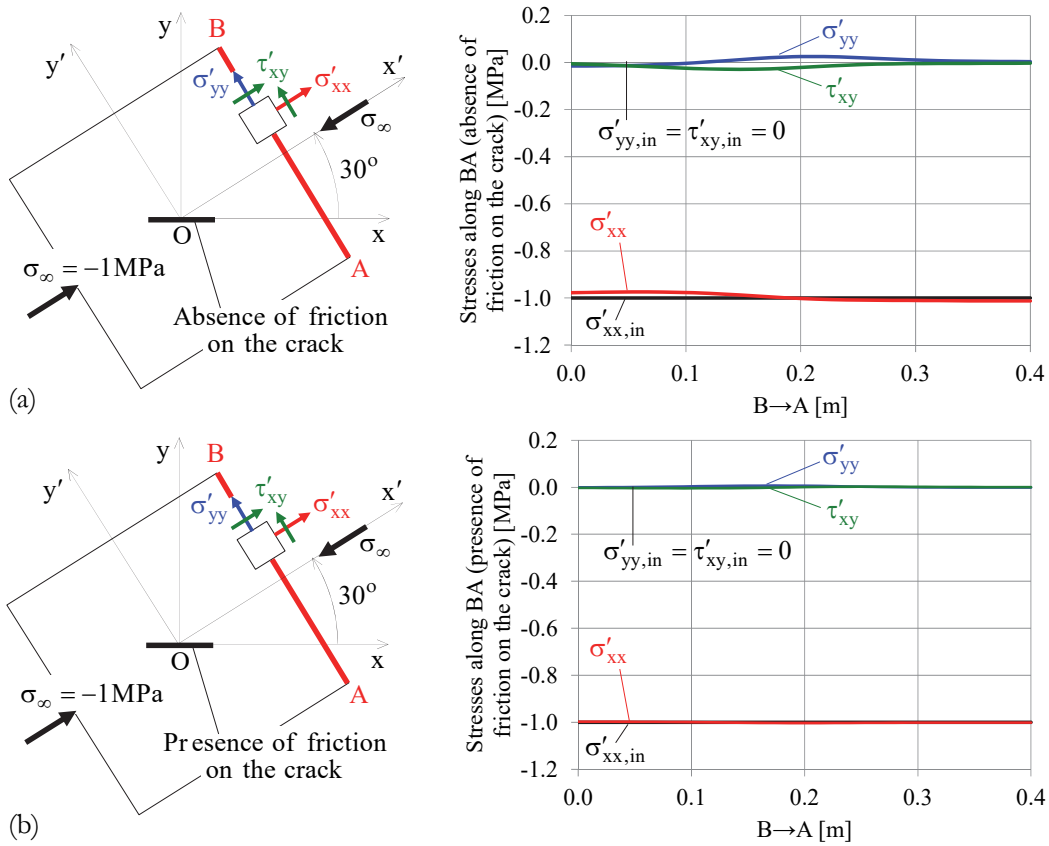


Figure 10: Stresses along BA for intact and cracked plates in case of (a) absence and (b) presence of friction along the crack lips.

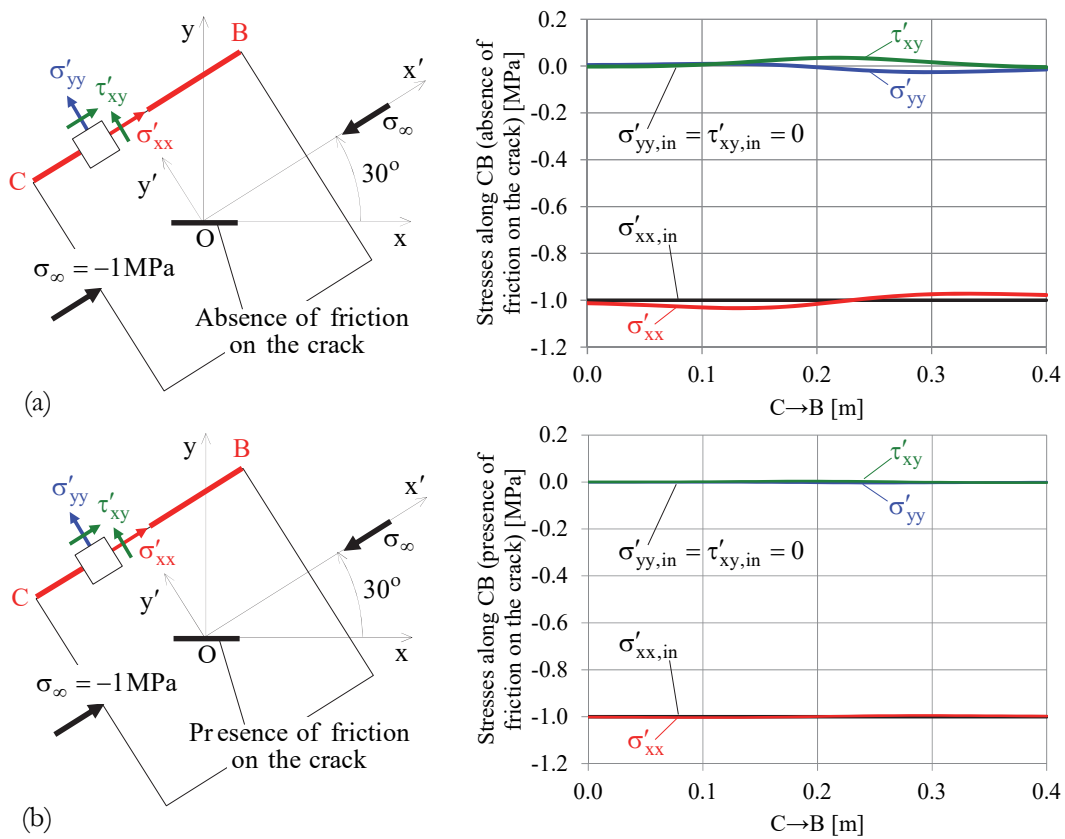


Figure 11: Stresses along CB for intact and cracked plates in case of (a) absence and (b) presence of friction along the crack lips.

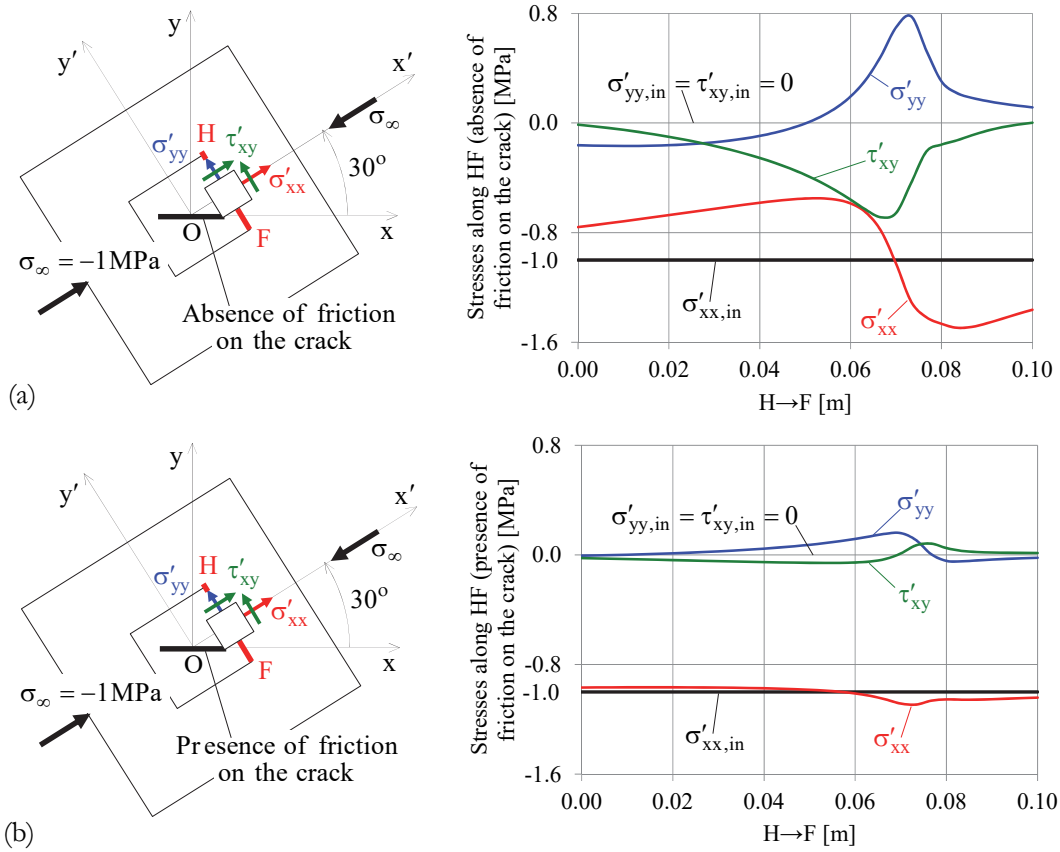


Figure 12: Stresses along HF for intact and cracked plates in case of (a) absence and (b) presence of friction along the crack lips.

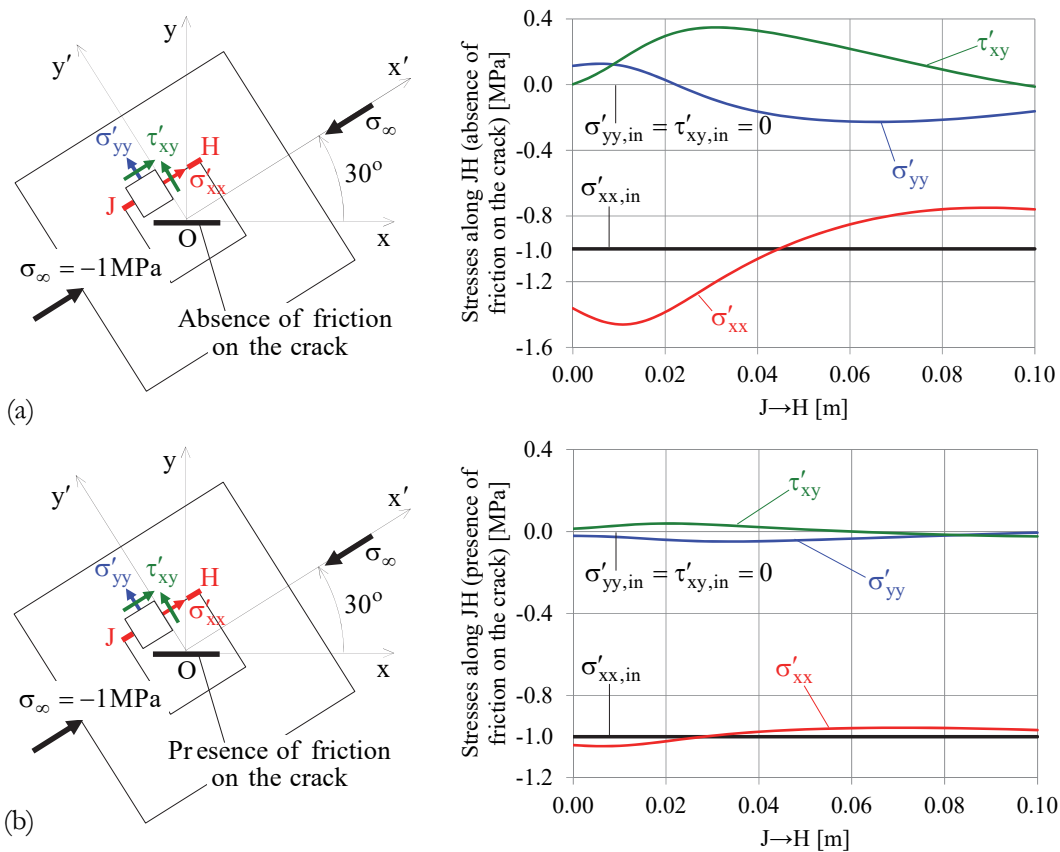


Figure 13: Stresses along JH for intact and cracked plates in case of (a) absence and (b) presence of friction along the crack lips.

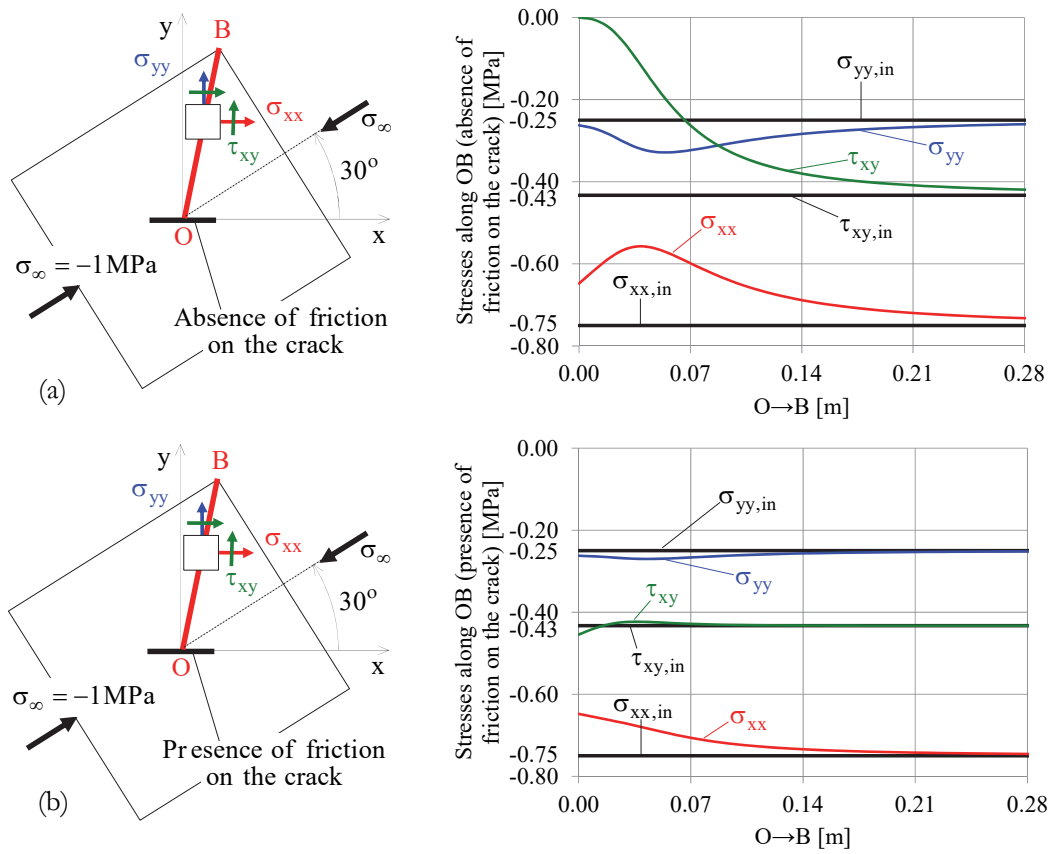


Figure 14: Stresses along the diagonal OB for intact and cracked plates in (a) absence and (b) presence of friction along the crack lips.

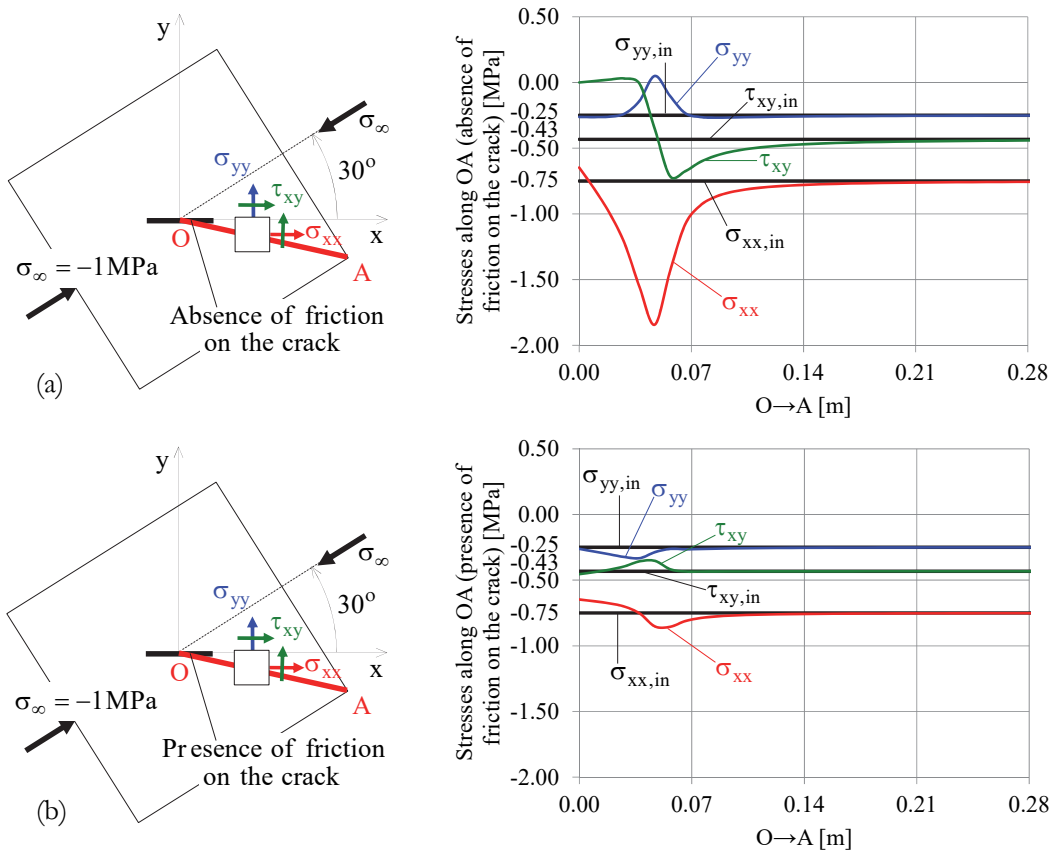


Figure 15: Stresses along the diagonal OA for intact and cracked plates in (a) absence and (b) presence of friction along the crack lips.



As it is seen from Figs.10 and 11, especially in the case of presence of friction with no relative sliding between the lips of the crack, the stresses for the cracked and these for the intact plates are almost identical on the boundaries of the plates, highlighting the potentiality of the ‘general solution’ of the infinite cracked plate presented in this study to describe approximately the problem of a cracked plate of finite dimensions, as well.

Moreover, from Fig.12 it can be concluded that the stresses in the vicinity of the crack are higher in the case of absence of friction with the maximum relative sliding between the lips of the crack. In both cases the stresses are maximized (concerning their absolute value) at around 2/3 of HF (i.e., closer to point F), which is the point of highest distortion of HF (see Fig.9b). Shear stress  $\tau_{xy}$  is zeroed at points H and F, in accordance with the deformed configuration of Fig.9b, from which it is seen that right angles at these points remain right after deformation. As previously, it is seen from Fig.13 that stresses in the vicinity of the crack are higher in the case of absence of friction. In both cases, as the left crack tip elevates (due to the clockwise crack rotation) the accumulation of material near the point J, causes in turn an increase in the compressive normal stress  $\sigma'_{xx}$ .

Concerning the perturbation of the stress field in the intact disc, due to the weakening of the plate by the crack, it is seen from Fig.14, that it is higher in the case of absence of friction (Fig.14a). In this case, the shear stress  $\tau_{xy}$  for the cracked plate is obviously zero at point O on the upper lip of the crack (since there is no friction). On the other hand, it is concluded that in the presence of friction (Fig.14b), all the stress components in the cracked plate attain values close to those of the intact plate, even on the crack itself. In general, the two stress fields (for the intact and the cracked plates) converge rapidly as one moves away from the crack (point O). Similar conclusions are drawn from Fig.15, regarding the stress field along the diagonal OA. In this case, since OA passes very closely from the right crack tip, the stresses in the cracked plate attain high absolute values at the projection of the crack tip on OA.

*Comparing the stress field on the crack lips and on the line 2a of the intact plate*

Of particular interest is the issue of the contact stresses developed between the lips of the crack. As it is concluded from Eqns.(33) and (34) the contact stresses are uniformly distributed along the lips of the crack. In addition, they depend on the material of the plate. Although this statement sounds strange, it is quite reasonable since the contact stresses result from a certain displacement field imposed to the crack lips in the ‘inverse problem’. Therefore they do depend on the material’s compliance: the lower the compliance the higher the stress field required to induce a definite boundary displacement.

In this context, the contact stresses on the crack lips are studied parametrically in juxtaposition to the respective stresses along a line 2a in the intact plate which do not depend on the plate’s material (as a result of a first fundamental problem in a simply connected region). For the problem of Fig.7a, i.e., for  $k=0$ , the contact stresses of Eqns.(33), (34) become:

$$\sigma_{yy}^{\pm} = \frac{(1+\kappa)^2 \sigma_{\infty}}{8\kappa} \delta \cdot (1 - \cos 2\beta), \quad \tau_{xy}^{\pm} = \frac{(1+\kappa)^2 \sigma_{\infty}}{8\kappa} \tau \cdot \sin 2\beta \tag{55, 56}$$

In the absence of friction, substituting from Eqns.(14) for  $\tau$  and  $\delta$  in Eqns.(55) and (56), yields:

$$\sigma_{yy}^{\pm} = \frac{(1+\kappa)^2 \sigma_{\infty}}{8\kappa} (\tan \lambda \cdot \tan \omega + 1)(1 - \cos 2\beta), \quad \tau_{xy}^{\pm} = 0 \tag{57}$$

where for plane strain,  $\tan \lambda = \tan \lambda(\beta, \sigma_{\infty}, E, \nu)$ :

$$\tan \lambda = \left| \frac{(1+\kappa) \sin 2\beta}{(1+\kappa) \cos 2\beta \sigma_{\infty} + 8\mu} \sigma_{\infty} \right| = \left| \frac{(1+3-4\nu) \sin 2\beta}{(1+3-4\nu) \cos 2\beta \sigma_{\infty} + \frac{4E}{1+\nu}} \sigma_{\infty} \right| = \left| \frac{(1-\nu^2) \sin 2\beta}{(1-\nu^2) \cos 2\beta \sigma_{\infty} + E} \sigma_{\infty} \right| \tag{58}$$

while for plane stress,  $\tan \lambda = \tan \lambda(\beta, \sigma_{\infty}, E)$ :

$$\tan \lambda = \left| \frac{(1+\kappa) \sin 2\beta}{(1+\kappa) \cos 2\beta \sigma_{\infty} + 8\mu} \sigma_{\infty} \right| = \left| \frac{\left(1 + \frac{3-\nu}{1+\nu}\right) \sin 2\beta}{\left(1 + \frac{3-\nu}{1+\nu}\right) \cos 2\beta \sigma_{\infty} + \frac{4E}{1+\nu}} \sigma_{\infty} \right| = \left| \frac{\sin 2\beta}{\cos 2\beta \sigma_{\infty} + 4E} \sigma_{\infty} \right| \tag{59}$$



Eqns. (58) and (59) indicate that, in the absence of friction, the normal contact stress depends always on Young’s modulus E through  $\tan\lambda$ , and on Poisson’s ratio  $\nu$  directly through  $\kappa=3-4\nu$  or  $\kappa=(3-\nu)/(1+\nu)$ , for plane strain or plane stress, respectively, and indirectly through  $\tan\lambda$  in the case of plane strain only ( $\tan\omega$  entering  $\delta$  does not depend on the material, as it is seen from Eqns.(11)). In the presence of friction, substituting for  $\tau$  and  $\delta$  from Eqns.(15) in Eqns.(55) and (56), yields:

$$\sigma_{yy}^{\pm} = \frac{(1+\kappa)^2 \sigma_{\infty}}{8\kappa} (1 - \cos 2\beta),$$

$$\tau_{xy}^{\pm} = \frac{(1+\kappa)^2 \sigma_{\infty}}{8\kappa} \sin 2\beta$$
(60)

From the last formulae, it is seen that in the presence of friction, the contact stresses depend only on  $\nu$  through  $\kappa$ , and not on E. Using Eqns.(55-60), the contact stresses are next calculated for plane strain and plane stress conditions, in either absence or presence of friction, for various E and  $\nu$  values, against the crack inclination angle  $\beta$ . The results are tabulated and then diagrams are plotted showing the influence of various parameters of the ‘general problem’ on the magnitude of contact stresses versus the respective stresses on the line  $2\alpha$  of the intact plate. In this context, Table 1 refers to the values of the contact stresses and the respective stresses in the intact plate when both plates (intact and cracked) are under uniaxial compression with a uniform pressure  $\sigma_{\infty} = -1$  MPa under plane strain conditions. The modulus of elasticity of the material is kept fixed,  $E=3.2$  GPa (e.g. PMMA) while Poisson’s ratio  $\nu$  assumes the values  $\nu=0.1, 0.2, 0.3,$  and  $0.4$ . For each  $\nu$ -value, angle  $\beta$  assumes the values  $15^\circ, 30^\circ, 45^\circ, 60^\circ$  and  $90^\circ$ . In addition, a distinction is made between presence and absence (smooth contact) of friction on the lips of the crack. Tab. 2 is analogue of Tab. 1, for plane stress conditions.

$\beta$	Plane strain, E=3.2 GPa																	
	Intact plate stresses [MPa]		$\nu=0.1$				$\nu=0.2$				$\nu=0.3$				$\nu=0.4$			
	$\sigma_{yy}^{in}$	$\tau_{xy}^{in}$	Contact stresses [MPa]		Contact stresses													
(52)	(52)	Smooth	Friction	Smooth	Friction	Smooth	Friction	Smooth	Friction	Smooth	Friction	Smooth	Friction	Smooth	Friction	Smooth	Friction	
	$\sigma_{yy}^{in}$	$\tau_{xy}^{in}$	$\sigma_{yy}^{\pm}$	$\tau_{xy}^{\pm}$	$\sigma_{yy}^{\pm}$	$\tau_{xy}^{\pm}$	$\sigma_{yy}^{\pm}$	$\tau_{xy}^{\pm}$	$\sigma_{yy}^{\pm}$	$\tau_{xy}^{\pm}$	$\sigma_{yy}^{\pm}$	$\tau_{xy}^{\pm}$	$\sigma_{yy}^{\pm}$	$\tau_{xy}^{\pm}$	$\sigma_{yy}^{\pm}$	$\tau_{xy}^{\pm}$	$\sigma_{yy}^{\pm}$	$\tau_{xy}^{\pm}$
	(52)	(52)	(57)	(57)	(60)	(60)	(57)	(57)	(60)	(60)	(57)	(57)	(60)	(60)	(57)	(57)	(60)	(60)
15°	-0.07	-0.25	-0.15	0.00	-0.08	-0.31	-0.14	0.00	-0.08	-0.29	-0.13	0.00	-0.07	-0.27	-0.11	0.00	-0.07	-0.26
30°	-0.25	-0.43	-0.56	0.00	-0.31	-0.54	-0.51	0.00	-0.29	-0.50	-0.47	0.00	-0.27	-0.47	-0.42	0.00	-0.26	-0.45
45°	-0.50	-0.50	-1.12	0.00	-0.62	-0.62	-1.02	0.00	-0.58	-0.58	-0.93	0.00	-0.54	-0.54	-0.84	0.00	-0.51	-0.51
60°	-0.75	-0.43	-1.68	0.00	-0.94	-0.54	-1.54	0.00	-0.87	-0.50	-1.39	0.00	-0.82	-0.47	-1.26	0.00	-0.77	-0.45
75°	-0.93	-0.25	-2.08	0.00	-1.16	-0.31	-1.91	0.00	-1.09	-0.29	-1.73	0.00	-1.02	-0.27	-1.57	0.00	-0.96	-0.26
90°	-1.00	0.00	-2.23	0.00	-1.25	0.00	-2.05	0.00	-1.16	0.00	-1.86	0.00	-1.09	0.00	-1.68	0.00	-1.03	0.00

Table 1: Contact stresses along the crack lips and the respective stresses in the intact plate (plane strain conditions).

$\beta$	Plane stress, E=3.2 GPa																	
	Intact plate stresses [MPa]		$\nu=0.1$				$\nu=0.2$				$\nu=0.3$				$\nu=0.4$			
	$\sigma_{yy}^{in}$	$\tau_{xy}^{in}$	Contact stresses [MPa]		Contact stresses													
(52)	(52)	Smooth	Friction	Smooth	Friction	Smooth	Friction	Smooth	Friction	Smooth	Friction	Smooth	Friction	Smooth	Friction	Smooth	Friction	
	$\sigma_{yy}^{in}$	$\tau_{xy}^{in}$	$\sigma_{yy}^{\pm}$	$\tau_{xy}^{\pm}$	$\sigma_{yy}^{\pm}$	$\tau_{xy}^{\pm}$	$\sigma_{yy}^{\pm}$	$\tau_{xy}^{\pm}$	$\sigma_{yy}^{\pm}$	$\tau_{xy}^{\pm}$	$\sigma_{yy}^{\pm}$	$\tau_{xy}^{\pm}$	$\sigma_{yy}^{\pm}$	$\tau_{xy}^{\pm}$	$\sigma_{yy}^{\pm}$	$\tau_{xy}^{\pm}$	$\sigma_{yy}^{\pm}$	$\tau_{xy}^{\pm}$
	(52)	(52)	(57)	(57)	(60)	(60)	(57)	(57)	(60)	(60)	(57)	(57)	(60)	(60)	(57)	(57)	(60)	(60)
15°	-0.07	-0.25	-0.15	0.00	-0.08	-0.31	-0.14	0.00	-0.08	-0.30	-0.14	0.00	-0.08	-0.29	-0.13	0.00	-0.07	-0.28
30°	-0.25	-0.43	-0.57	0.00	-0.31	-0.54	-0.54	0.00	-0.30	-0.52	-0.51	0.00	-0.29	-0.49	-0.50	0.00	-0.28	-0.48
45°	-0.50	-0.50	-1.13	0.00	-0.63	-0.63	-1.07	0.00	-0.60	-0.60	-1.03	0.00	-0.57	-0.57	-0.99	0.00	-0.55	-0.55
60°	-0.75	-0.43	-1.70	0.00	-0.94	-0.54	-1.61	0.00	-0.89	-0.52	-1.54	0.00	-0.86	-0.49	-1.49	0.00	-0.82	-0.48
75°	-0.93	-0.25	-2.11	0.00	-1.17	-0.31	-2.00	0.00	-1.11	-0.30	-1.92	0.00	-1.06	-0.29	-1.85	0.00	-1.03	-0.28
90°	-1.00	0.00	-2.26	0.00	-1.25	0.00	-2.15	0.00	-1.19	0.00	-2.06	0.00	-1.14	0.00	-1.98	0.00	-1.10	0.00

Table 2: Contact stresses along the crack lips and the respective stresses in the intact plate (plane stress conditions).

Using the data of Tabs. 1 and 2, diagrams can be drawn, exhibiting the influence of the above mentioned parameters on the stress field along the crack lips and along the line  $2\alpha$  of the intact plate (see Figs.16 and 17).

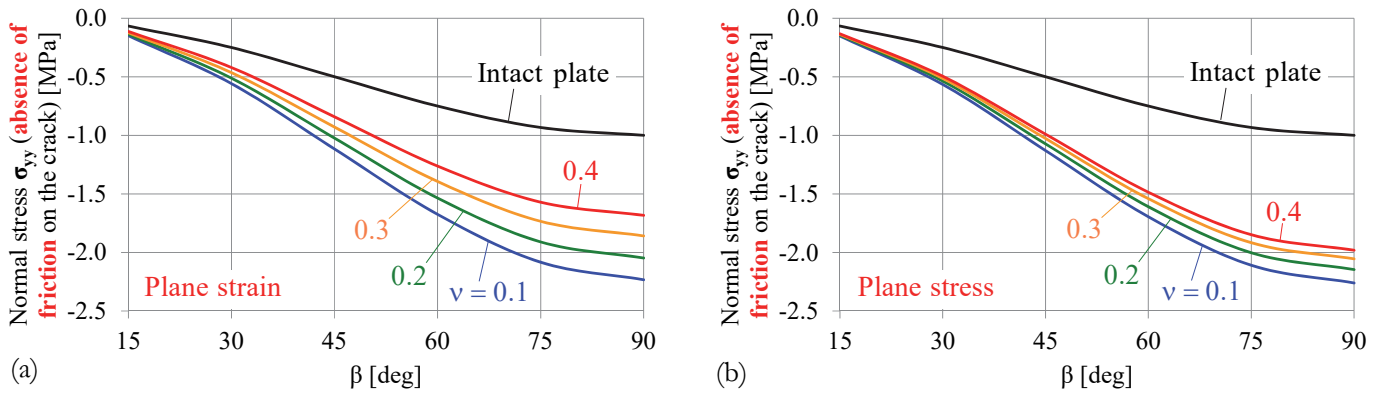


Figure 16: Variation of the  $\sigma_{yy}$  stress (contact stresses  $\sigma_{yy}^{\pm}$  in the cracked plate and the respective stresses  $\sigma_{yy}^{in}$  in the intact one) versus angle  $\beta$ , for various  $\nu$ -values, in case of smooth contact between the crack lips, for (a) plane strain and (b) plane stress conditions.

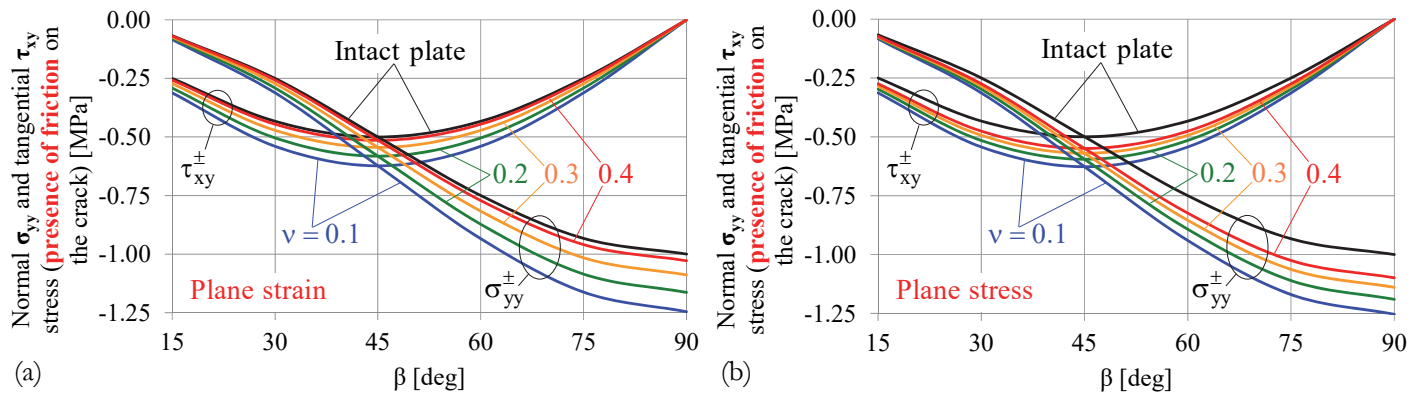


Figure 17: Variation of the  $\sigma_{yy}$  and  $\tau_{xy}$  stresses (contact stresses in the cracked plate and the respective ones in the intact plate) versus angle  $\beta$ , for various  $\nu$ -values, in case of frictional contact between the crack lips, for (a) plane strain and (b) plane stress conditions.

As it is seen from Fig.16, in the absence of friction between the lips of the crack, the contact stress  $\sigma_{yy}^{\pm}$  is significantly affected by Poisson's ratio and by increasing angle  $\beta$ , exceeding always the respective stress  $\sigma_{yy}^{in}$  in the intact plate. The differences among  $\sigma_{yy}^{\pm}$ , regarding the variation of  $\nu$ , are more pronounced for plane strain conditions. On the other hand, the biggest difference between  $\sigma_{yy}^{\pm}$  and  $\sigma_{yy}^{in}$  appears for plane stress conditions (recall that, as already highlighted,  $\sigma_{yy}^{in}$  is insensitive to plane strain or plane stress conditions) reaching up to 226% for  $\nu=0.1$  at  $\beta=90^\circ$ .

Fig.17 is analogous to Fig.16 for the case of friction between the lips of the crack. In this case, apart from  $\sigma_{yy}^{\pm}$ , shear contact stresses  $\tau_{xy}^{\pm}$  are, also, generated. It is seen from Fig.17, that the difference between  $\sigma_{yy}^{\pm}$  and  $\sigma_{yy}^{in}$  is smaller from the case of smooth contact between the crack lips, reaching, for either plane strain or plane stress conditions, values only up to 25% for  $\nu=0.1$  at  $\beta=90^\circ$ . For increasing Poisson's ratios and plain strain conditions  $\sigma_{yy}^{\pm}$  and  $\tau_{xy}^{\pm}$  tend to  $\sigma_{yy}^{in}$  and  $\tau_{xy}^{in}$ .

In order now to quantify the role of the modulus of elasticity  $E$ , the respective, as previously stresses, are calculated and listed in Tab. 3, for smooth contact between the lips of the crack, and for both plane strain and plane stress conditions for various values of  $E$  (equal to 5, 8, 15 and 100 GPa) and for a fixed value for Poisson's ratio, equal to  $\nu=0.3$ .

As mentioned before,  $E$  influences only the contact stress  $\sigma_{yy}^{\pm}$  and only in the case of absence of friction (see Eqns.(57-59)). Using the results of Tab. 3, the influence of Young's modulus  $E$  on the contact stress  $\sigma_{yy}^{\pm}$  in juxtaposition to  $\sigma_{yy}^{in}$  in the intact plate, is plotted in next Fig.18. It is concluded that the difference between plane strain and plane stress is small regarding the range of  $E$ -values considered, while for increasing  $E$ -values  $\sigma_{yy}^{\pm}$  tends to  $\sigma_{yy}^{in}$ .

$\beta$	Smooth contact between the crack lips, $\nu=0.3$																	
	Intact plate stresses [MPa]		E=5 GPa				E=8 GPa				E=15 GPa				E=100 GPa			
			Contact stresses [MPa]		Contact stresses													
	$\sigma_{yy}^{\text{in}}$	$\tau_{xy}^{\text{in}}$	Plane strain	Plane stress	Plane strain	Plane stress	Plane strain	Plane stress	Plane strain	Plane stress	Plane strain	Plane stress	Plane strain	Plane stress				
	$\sigma_{yy}^{\pm}$	$\tau_{xy}^{\pm}$	$\sigma_{yy}^{\pm}$	$\tau_{xy}^{\pm}$	$\sigma_{yy}^{\pm}$	$\tau_{xy}^{\pm}$	$\sigma_{yy}^{\pm}$	$\tau_{xy}^{\pm}$	$\sigma_{yy}^{\pm}$	$\tau_{xy}^{\pm}$	$\sigma_{yy}^{\pm}$	$\tau_{xy}^{\pm}$	$\sigma_{yy}^{\pm}$	$\tau_{xy}^{\pm}$	$\sigma_{yy}^{\pm}$	$\tau_{xy}^{\pm}$		
	(52)	(52)	(57)	(57)	(57)	(57)	(57)	(57)	(57)	(57)	(57)	(57)	(57)	(57)	(57)	(57)		
15°	-0.07	-0.25	-0.10	0.00	-0.11	0.00	-0.09	0.00	-0.10	0.00	-0.08	0.00	-0.09	0.00	-0.07	0.00		
30°	-0.25	-0.43	-0.38	0.00	-0.41	0.00	-0.34	0.00	-0.36	0.00	-0.31	0.00	-0.32	0.00	-0.28	0.00		
45°	-0.50	-0.50	-0.76	0.00	-0.83	0.00	-0.67	0.00	-0.72	0.00	-0.61	0.00	-0.65	0.00	-0.55	0.00		
60°	-0.75	-0.43	-1.15	0.00	-1.24	0.00	-1.01	0.00	-1.08	0.00	-0.91	0.00	-0.97	0.00	-0.83	0.00		
75°	-0.93	-0.25	-1.43	0.00	-1.54	0.00	-1.26	0.00	-1.34	0.00	-1.14	0.00	-1.20	0.00	-1.03	0.00		
90°	-1.00	0.00	-1.53	0.00	-1.65	0.00	-1.35	0.00	-1.44	0.00	-1.22	0.00	-1.29	0.00	-1.11	0.00		

Table 3: Contact stresses along the crack lips and the respective stresses in the intact plate (plane stress conditions).

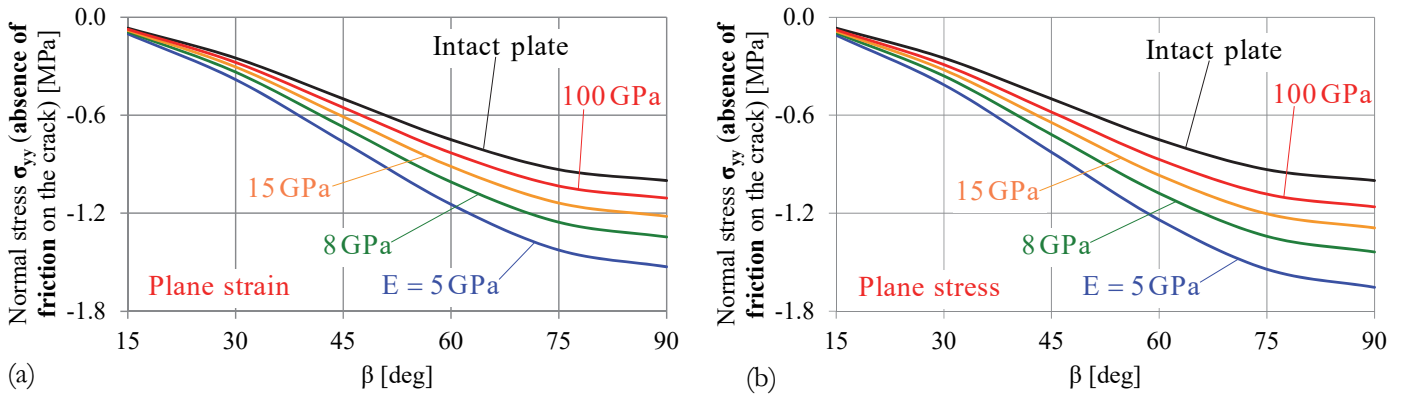


Figure 18: Variation of the  $\sigma_{yy}$  stress (contact stresses  $\sigma_{yy}^{\pm}$  in the cracked plate and the respective stresses  $\sigma_{yy}^{\text{in}}$  in the intact plate) against angle  $\beta$ , for various Young's moduli  $E$  and for a fixed Poisson's ratio  $\nu$ , in case of smooth contact between the crack lips, for: (a) plane strain and (b) plane stress conditions.

*The SIFs for the 'general problem' in the uniaxially compressed cracked plate*

Clearly, SIFs have no meaning in the case of presence of friction on the crack which here is associated with completely stuck lips, since in this case Eqns.(47) and (48) yield immediately  $K_I=K_{II}=0$ . Thus, only the case of absence of friction will be examined. However, not only the case  $\tau=0$  of Eqns.(14) is considered, but values in the whole  $[0,1]$  range, are assigned to  $\tau$ . It is assumed that energy conservation is satisfied due to the zero friction coefficient between the lips of the crack, so that the more general conditions of Eqns.(13) will hold for  $\tau$  and  $\delta$ . Under the above assumption, and for  $k=0$ , Eqns.(47) and (48) for the SIFs become:

$$K_I = -\frac{\sigma_{\infty} \sqrt{\pi\alpha}}{2} (1-\tau) \cdot \tan \lambda \cdot \tan \omega \cdot (1-\cos 2\beta) \tag{61}$$

$$K_{II} = \frac{\sigma_{\infty} \sqrt{\pi\alpha}}{2} (1-\tau) \sin 2\beta, \quad 0 \leq \tau < 1 \tag{62}$$

In addition, the study will be limited to plain strain condition, regarding the general fact that only in this case SIFs may be considered as a constant material property. Taking into account Eqn.(58) and the second of Eqns.(11), Eqn.(61) becomes:

$$K_I = -\frac{\sigma_{\infty} \sqrt{\pi\alpha}}{2} (1-\tau) \left| \frac{(1-\nu^2) \sin 2\beta}{(1-\nu^2) \cos 2\beta \sigma_{\infty} + E} \right| \sigma_{\infty} \sin 2\beta = -K_{II} \tan \lambda \tag{63}$$

From the above formulae, it is seen that  $K_I$  apart from  $\alpha$ ,  $\sigma_\infty$  and  $\beta$ , depends also on the material (i.e., on  $\nu$  and  $E$ ), while  $K_{II}$  is material independent. In this context, the variation of  $K_I$  against  $\nu$  is plotted in Fig.19a. To plot  $K_I(\nu)$ ,  $E$  was kept fixed equal to 3.2 GPa (PMMA), while it was assumed that  $\sigma_\infty = -1$  MPa,  $\tau = 0$ , and  $\beta = 45^\circ$  (at which  $K_I$  assumes its maximum value). In Fig.19b,  $K_I$  is plotted against  $E$  for the as above  $\sigma_\infty$ ,  $\tau$  and  $\beta$ . In this case,  $\nu$  was kept fixed equal to 0.3.

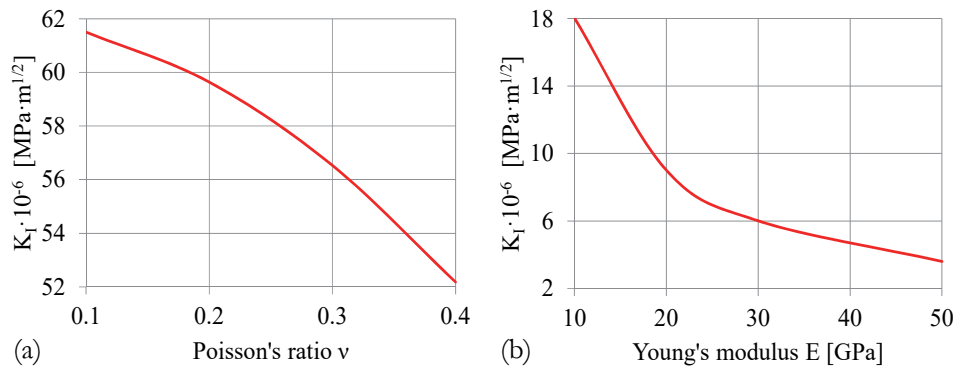


Figure 19: The variation of  $K_I$  at the crack tip, for  $\sigma_\infty = -1$  MPa,  $\tau = 0$ , and  $\beta = 45^\circ$ : (a) against  $\nu$ , for a fixed  $E = 3.2$  GPa, and (b) against  $E$ , for a fixed  $\nu = 0.3$ .

It should be noticed, however, that  $K_I$  assumes extremely small values compared to  $K_{II}$  since  $\tan\lambda$  is a very small quantity. Actually, for  $\beta = 0^\circ$ ,  $K_I$  vanishes, in accordance with the zero crack opening displacement (see the second of Eqns.(9) or of Eqns.(43), for  $k=0$  and  $\beta=0^\circ$ ). For  $\beta = 90^\circ$ ,  $K_I$  vanishes as well, because  $\lambda$  vanishes. For all other values, i.e., for  $0^\circ < \beta < 90^\circ$  (in case the cracked plate is under uniaxial compression, i.e.,  $k=0$ ),  $K_I$  assumes (very small) finite positive values, so that, upon combined with the negative  $K_{II}$ -values it suffices full contact of the crack lips. Assuming again that  $E = 3.2$  GPa,  $\nu = 0.36$ , and  $\sigma_\infty = -1$  MPa,  $K_I$  and  $K_{II}$  are plotted, for various values of  $\tau$ , against  $\beta$  in Fig.20a.  $K_I$  values are only visible in the magnified view of Fig.20b. As mentioned previously,  $K_I$  attains its maximum values at  $\beta = 45^\circ$ . In Fig.20a, the unnatural case of negative  $K_I$  (corresponding to the unnatural overlapping) is also shown for overview reasons.

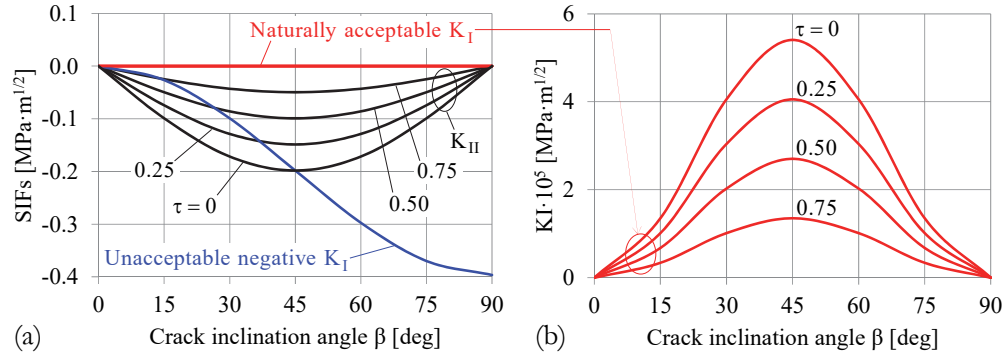


Figure 20: (a) The naturally unacceptable negative  $K_I$ -value for a uniaxially compressed cracked plate, and the variation of the naturally acceptable  $K_I$ - and  $K_{II}$ -values due to the ‘general problem’, for various  $\tau$ -values, against the crack inclination angle  $\beta$ . (b) A magnified view of the naturally acceptable  $K_I$ -values.

The findings of the present analysis regarding SIFs are in qualitative agreement with existing approaches addressing overlapping [29-31], but here, in particular for uniaxial compression of the cracked plate,  $K_{II}$  is always accompanied with normal contact stresses on the crack.

## DISCUSSION AND CONCLUSIONS

Some classical concepts of LFM were revisited in this study, in the light of a novel approach for quantifying the contact stresses developed on the lips of a ‘mathematical’ crack in an elastic plate, in case the crack lips are forced to mutual contact against each other. The inconsistency of this configuration with the classical solution of plane LFM, prohibits determination of these contact stresses (recall the boundary condition of stress free crack lips), leading to unnatural overlapping of the crack lips, and, moreover to unnatural negative values for the mode-I SIF.

The present study was based on a previous work (the so-called ‘initial problem’) according to which both components of the displacement vector of the points lying on the crack lips consist of two terms: a linear and an elliptic one. The linear terms lead to a naturally acceptable rotation and length alteration of the crack while the elliptic terms lead to either opening of the crack lips or to their overlapping, with the latter case being (obviously) physically unacceptable.

In this work, the unnatural overlapping was addressed by properly inverting the elliptic terms of the displacements, keeping the linear terms in their original form (i.e., as provided by the traditional LEFM solution of the ‘initial problem’). This was implemented by superposing to the incorrect (in the case of overlapping) solution of the ‘initial problem’ the solution of a mixed fundamental problem, denoted as the ‘inverse problem’. The superposition leads to the so-called ‘general problem’, which is able to provide natural solutions either for open or closing cracks.

In this context, the contact stresses developed on the lips of the crack, when they are forced to mutual contact against each other, were estimated and the role of several parameters on the magnitude of these contact stresses was quantified. These parameters were: (a) the state of stress and deformation, i.e., plane stress or plane strain, (b) the absence or presence of friction between the crack lips, (c) the Poisson’s ratio  $\nu$ , (d) the Young’s modulus  $E$  and (e) the crack inclination angle  $\beta$  with respect to the direction of the uniaxial compression of the crack plate.

The parametric analysis of the displacement and stress fields of the cracked plate was made in parallel with the respective analysis for an intact plate under identical loading schemes, for comparison reasons. It was, once again, verified that the solution of the ‘general problem’ for the infinite cracked plate may be satisfactorily adopted in the case of a finite centrally cracked plate with no further modifications.

Another interesting result was that the contact stresses developed on the crack  $2\alpha$  exceed always (and sometimes significantly) the respective stresses calculated along the line  $2\alpha$  in the intact plate, which at a first glance might sound strange.

For example, the normal contact stress  $\sigma_{yy}^{\pm}$  was found to be 2.23 times the respective  $\sigma_{yy}^{in}$  stress in the intact plate, when  $\beta=90^\circ$ , i.e., the load is normal to the crack, and the Poisson’s ratio equal to  $\nu=0.1$  (Fig.16a, Tab. 1). In another example (Fig.18a, Tab. 3), it was shown that for the smallest value considered for the Young’s modulus (i.e., for  $E=5$  GPa), the contact stress  $\sigma_{yy}^{\pm}$  was 1.53 times the respective  $\sigma_{yy}^{in}$  stress in the intact plate, when  $\beta=90^\circ$ . To further clarify this point, one must consider that  $\beta=90^\circ$  and  $k=0$  in the first of Eqns.(43) and Eqns.(53). Assuming, in addition, plane strain conditions the displacement components of the crack lips along the crack axis, and those of the line  $2\alpha$  in the intact plate, are obtained respectively as:

$$u^{\pm}(x) = -\frac{(1+\nu)\sigma_{\infty}}{8\mu}x = -\frac{(1+3-4\nu)\sigma_{\infty}}{8\mu}x = -\frac{(1-\nu)\sigma_{\infty}}{2\mu}x \tag{64}$$

$$u_{in}(x) = -\frac{(3-\nu)\sigma_{\infty}}{8\mu}x = -\frac{(3-3+4\nu)\sigma_{\infty}}{8\mu}x = -\frac{\nu\sigma_{\infty}}{2\mu}x \tag{65}$$

Let us examine first the role of Poisson’s ratio  $\nu$ . As it is seen from Eqns.(64) and (65) the span of the crack and the line  $2\alpha$  of the intact plate after deformation could only be equal for  $\nu=0.5$  (so that  $u^{\pm}(x) = u_{in}(x)$ ), which cannot be the case under the linear elastic assumption adopted in this study. For  $\nu<0.5$ ,  $u^{\pm}(x)$  is always bigger than  $u_{in}(x)$ , so the span of the deformed crack will always exceed that of the segment  $2\alpha$ . This is clearly seen in Fig.21, in which the deformed configurations of the cracked and the intact plate (for a very high value of  $\sigma_{\infty}$  for clarity) are shown in juxtaposition to each other. It is to be mentioned, that while the dilatation of the plate ABCD along the x-direction (due to Poisson’s effect) is almost identical for the cracked and the intact plates (Fig.21a), the dilatation of the internal square FHJN, enclosing the crack/line  $2\alpha$ , is locally, along axis x, higher in the case of the cracked plate (Fig.21b). For this to be true, a higher normal contact pressure should apply to the crack with respect to that on the line  $2\alpha$  in the intact plate. What is more, as it follows from Eqns.(64) and (65), the smaller the  $\nu$  the larger the span of the crack after deformation (equal to the local dilatation of the square FHJN along x-axis) with respect to the span of the line  $2\alpha$ . This explains why for decreasing  $\nu$ -values, an increasing normal contact stress is required in the cracked plate, compared to the respective normal stress in the intact one. Regarding the role of the modulus of elasticity  $E$ , substituting  $E(1+\nu)$  for  $2\mu$  in Eqns.(64) and (65) yields:

$$u^{\pm}(x) = -\frac{(1-\nu^2)\sigma_{\infty}}{E}x \tag{66}$$

$$u_{in}(x) = -\frac{\nu(1+\nu)\sigma_{\infty}}{E}x \tag{67}$$

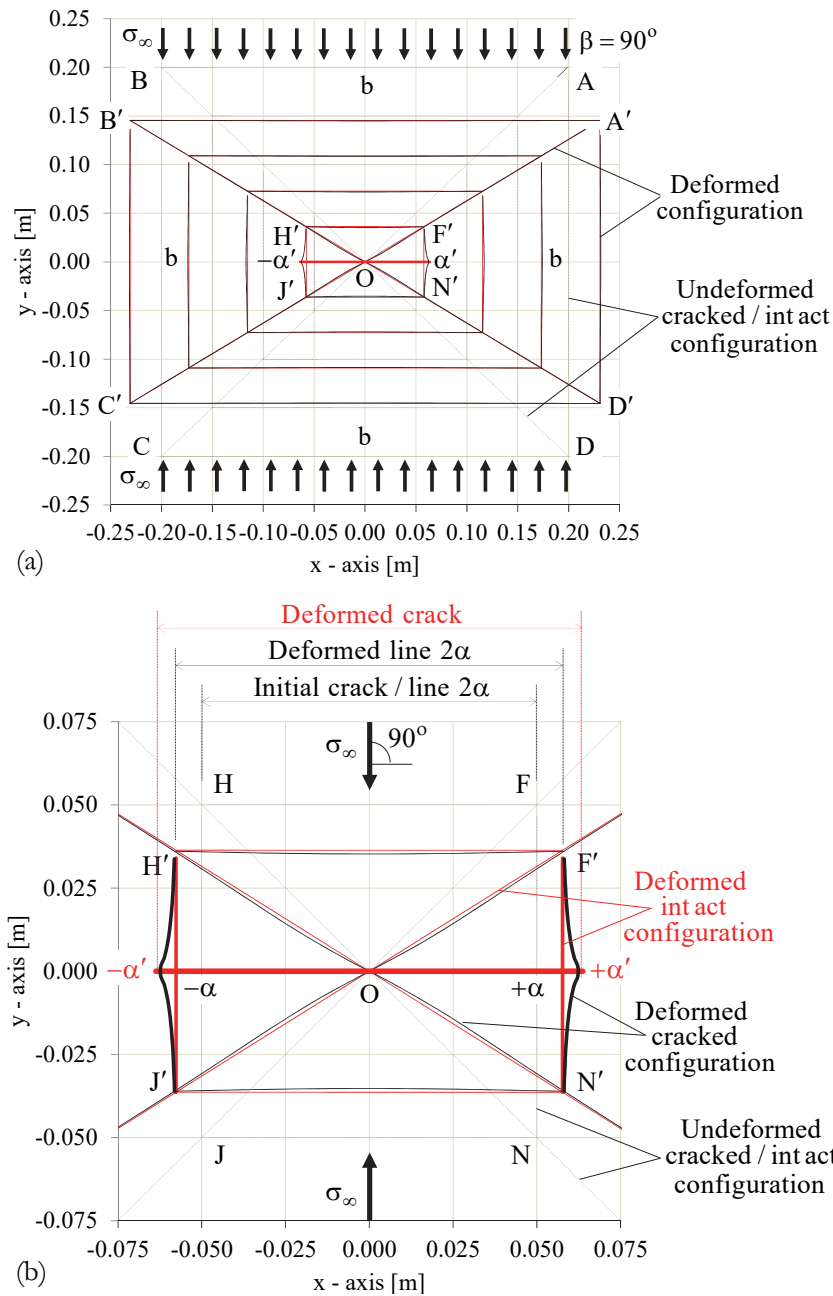


Figure 21: a) The deformed versus the undeformed configurations of the cracked and the intact square plates under uniaxial pressure normal ( $\beta=90^\circ$ ) to the crack/line  $2\alpha$ . (b) Magnified view of the crack area.

It is once again concluded that the span of the crack and the line  $2\alpha$  of the intact plate after deformation are equal only when  $\nu=0.5$  which cannot be the case. For  $\nu<0.5$ ,  $u^\pm(x)$  is always bigger than  $u_{in}(x)$  so that the span of the deformed crack will always exceed that of the line  $2\alpha$ . What is more, for any fixed value of  $\nu<0.5$ , it is easily seen that by decreasing  $E$ , the difference between  $u^\pm(x)$  and  $u_{in}(x)$  increases, explaining why for decreasing  $E$ -values, an increasing normal contact stress is required in the cracked plate, compared to the respective normal stress in the intact one.

It is here emphasized that what is discussed regarding the fact that  $(\sigma_{yy}^\pm, \tau_{xy}^\pm) > (\sigma_{yy}^{in}, \tau_{xy}^{in})$ , is a consequence of the basic assumption of the present study that the linear terms of the displacements provided by the traditional solution of the 'initial problem' of LEFM were accepted "as they are". However this an assumption that must be further explored and validated, because if  $\sigma_{yy}^\pm, \tau_{xy}^\pm$  were to be equal to  $\sigma_{yy}^{in}, \tau_{xy}^{in}$ , then  $u^\pm, v^\pm$  should tend to  $u_{in}, v_{in}$  of the intact plate. This is the subject of an ongoing research project implemented according to a combined experimental and analytic manner.



Before concluding it is worth considering briefly the issue of the pure mode-II SIF (an issue commonly discussed in literature in the form of the question “is it possible to implement pure mode-II loading schemes?”) taking advantage of the analytical solution presented in this study. Indeed, according to the ‘initial problem’, pure  $K_{II}$  conditions are obtained by setting in Eqns.(12)  $k=-1$  and  $\beta=45^\circ$ , whence:

$$K_{I,(1)} = 0, \quad K_{II,(1)} = \sigma_\infty \sqrt{\pi\alpha} \quad (\sigma_\infty < 0) \tag{68}$$

However, in this case Eqns.(9) yield overlapping lips:

$$v_1^\pm(x) = \frac{(1+\kappa)\sigma_\infty}{4\mu} x \tag{69}$$

$$u_1^\pm(x) = \pm \frac{(1+\kappa)\sigma_\infty}{4\mu} \sqrt{\alpha^2 - x^2} \tag{70}$$

Namely, the crack expands and rotates about the origin due to Eqn.(69) and from this position the one lip passes over the other in x-direction due to Eqn.(70). On the other hand, according to the ‘general problem’, pure  $K_{II}$  conditions are obtained by setting in Eqns.(47) and (48)  $k=-1$  and  $\beta=45^\circ$ , whence:

$$K_I = 0, \quad K_{II} = \sigma_\infty \sqrt{\pi\alpha}(1-\tau) \tag{71}$$

But in the ‘general problem’ one must put  $\tau=1$  to prevent overlapping, in which case the second one of Eqns.(71) yields  $K_{II}=0$ , i.e., the ‘general problem’ cannot provide pure mode-II SIF. However, in the frame of the ‘general problem’, a set of values for  $K_{II}$  and  $K_I$  fulfilling the conditions of Eqns.(68) may always be obtained, even approximately. Namely, in the case of a uniaxially compressed plate ( $k=0$ ) with a central short crack at an angle  $\beta=45^\circ$  with respect to the compressive stress  $\sigma_\infty$ , and zero friction ( $\tau=0$ ) between the lips of the crack (a relatively easy-to-achieve condition during a laboratory experiment), Eqns.(62) and (61 or 63) yield respectively (see Fig.(20)):

$$K_{II} = \frac{\sigma_\infty \sqrt{\pi\alpha}}{2} \tag{72}$$

$$K_I = -\frac{\sigma_\infty \sqrt{\pi\alpha}}{2} \left| \frac{(1-\nu^2)\sin 2\beta}{(1-\nu^2)\cos 2\beta\sigma_\infty + E} \right| = -K_{II} \tan \lambda \tag{73}$$

$\tan \lambda$

Definitely, the similarity between Eqs.(72, 73) and (68) by no means implies pure mode-II conditions. The SIFs given by Eqns.(72, 73) correspond to shearing stress  $\sigma_\infty/2$  parallel to the crack accompanied by biaxial pressure  $\sigma_\infty/2$  along and normal to the crack, leading to noticeable normal contact stresses on the crack lips, equal, according to Eqns.(34) and (14), to:

$$\sigma_{yy}^\pm = \frac{(1+\kappa)^2 \sigma_\infty}{8\kappa} \delta \tag{74}$$

Coming to an end, it can be stated that, LEFM (although it may be characterized, perhaps, outdated or out of fashion) it remains a quite valuable tool for the Structural Engineering community, providing important information about critical problems, related to the integrity of structures and structural elements in case they are weakened by discontinuities in the form of cracks. Although the concepts considered in this paper (i.e., ‘mathematical’ crack, infinite plate and the respective SIFs) are of relatively limited practical applicability (the size of actual structural members is by no means infinite and the discontinuities cannot be considered as ‘mathematical’ cracks with singular tips, and therefore the respective stress fields cannot be described by the traditional concept of SIFs), the analysis here presented, if properly adjusted, would provide equally interesting results for actual structures, as it will be proven in the next two papers of this three-paper series.



## ACKNOWLEDGEMENTS

The present paper is based on the Plenary Lecture entitled “Quantifying elastic contact stresses on the lips of ‘mathematical’ cracks”, given by the second author (Stavros K. Kourkoulis), on the occasion of awarding to him the “Paolo Lazzarin Medal” of the Italian Group of Fracture (IGF), during the “27<sup>th</sup> International Conference on Fracture and Structural Integrity”, organized by the IGF, from February 21 to February 24, 2023 at Rome (Italy).

## REFERENCES

- [1] Nui, L.S., Chehimi, C. and Pluvillage, G. (1994). Stress field near a large blunted tip V-notch and application of the concept of the critical notch stress intensity factor (NSIF) to the fracture toughness of very brittle materials, *Eng. Fract. Mech.*, 49(3), pp. 325-335. DOI: 10.1016/0013-7944(94)90262-3.
- [2] Lazzarin, P. and Filippi, S. (2006). A generalized stress intensity factor to be applied to rounded V-shaped notches. *Int. J. Solids Struct.*, 43(9), 2461-2478. DOI: 10.1016/j.ijsolstr.2005.03.007.
- [3] Gómez, F.J., Elices, M., Berto, F. and Lazzarin, P. (2008). A generalized notch stress intensity factor for U-notched components loaded under mixed mode, *Eng. Fract. Mech.*, 75(16), pp. 4819-4833. DOI: 10.1016/j.engfracmech.2008.07.001
- [4] Berto, F. and Lazzarin, P. (2009). A review of the volume-based strain energy density approach applied to V-notches and welded structures, *Theor. Appl. Fract. Mech.*, 52(3), pp. 183-194. DOI: 10.1016/j.tafmec.2009.10.001
- [5] Torabi, A.R., Bahrami, B. and Ayatollahi, M.R. (2019). Experimental determination of the notch stress intensity factor for sharp V-notched specimens by using the digital image correlation method, *Theor. Appl. Fract. Mech.*, 103, 102244. DOI: 10.1016/j.tafmec.2019.102244.
- [6] Burniston, E.E. (1969). An example of a partially closed Griffith crack, *Int. J. Fract. Mech.*, 5, pp. 17–24. DOI: 10.1007/BF00189935
- [7] Tweed, J. (1970). The determination of the stress intensity factor of a partially closed Griffith crack, *Int. J. Eng. Sci.*, 8(9), pp. 793-803. DOI: 10.1016/0020-7225(70)90005-4
- [8] Thresher, R.W. and Smith, F.W. (1973). The partially closed Griffith crack, *Int. J. Fract.*, 9, pp. 33-41. DOI: 10.1007/BF00035953.
- [9] Burniston, E.E. and Gurley, W.Q. (1973). The effect of partial closure on the stress intensity factor of a Griffith crack opened by a parabolic pressure distribution, *Int. J. Fract.*, 9, pp. 9-19. DOI: 10.1007/BF00035951.
- [10] Aksogan, O. (1975). Partial closure of a Griffith crack under a general loading, *Int. J. Fract.*, 11, 659-670. DOI: 10.1007/BF00116373.
- [11] Bowie, O.L. and Freese, C.E. (1976). On the “overlapping” problem in crack analysis, *Eng. Fract. Mech.*, 8(2), pp. 373-379. DOI: 10.1016/0013-7944(76)90017-5.
- [12] Dundurs, J. and Comninou, M. (1983). On the exterior crack with contact zones, *Int. J. Eng. Sci.*, 21(3), pp. 223-230. DOI: 10.1016/0020-7225(83)90024-1.
- [13] Theocaris, P.S., Papis, D. and Konstantellos, B.D. (1986). The exact shape of a deformed internal slant crack under biaxial loading, *Int. J. Fract.*, 30, pp. 135-153. DOI: 10.1007/BF00034022.
- [14] Papis, D., Theocaris, P.S. and Konstantellos, B. (1988). Elastic overlapping of the crack flanks under mixed-mode loading, *Int. J. Fract.*, 37, pp. 303-319. DOI: 10.1007/BF00032535.
- [15] Theocaris, P.S. and Sakellariou, M. (1991). A correction model for the incompatible deformations of the shear internal crack, *Eng. Fract. Mech.*, 38, pp. 231-240. DOI: 10.1016/0013-7944(91)90001-H.
- [16] Beghini, M. and Bertini, L. (1996). Effective stress intensity factor and contact stress for a partially closed Griffith crack in bending. *Eng. Fract. Mech.*, 54(5), 667-678. DOI: 10.1016/0013-7944(95)00234-0
- [17] Corrado, M., Carpinteri, A., Paggi, M. and Mancini, G. (2008). Improving in the plastic rotation evaluation by means of fracture mechanics concepts, In: Walraven, J.C., Stoelhorst, D., eds. *Tailor made concrete structures - New solutions for our society*. CRC Press/Balkema, The Netherlands, pp. 541-546.
- [18] Carpinteri, A., Corrado, M. and Paggi, M. (2010). An integrated cohesive/overlapping crack model for the analysis of flexural cracking and crushing in RC beams, *Int. J. Fract.*, 161, pp. 161-173. DOI: 10.1007/s10704-010-9450-4.
- [19] Chen, Y.Z., Lin, X.Y., Wang, Z.X. and Nik Long, N.M.A. (2008). Solution of contact problem for an arc crack using hypersingular integral equation, *Int. J. Comp. Methods*, 5(01), pp. 119-133. DOI: 10.1142/S0219876208001418.
- [20] Enescu, I. (2018). Stress intensity factors in crack closure problems, *Int. J. Theor. Appl. Mech.*, 3, pp. 49-55.



- [21] Antunes, F.V., Paiva, L., Branco, R. and Borrego, L.P. (2019). Effect of underloads on plasticity-induced crack closure: a numerical analysis, *J. Eng. Mater. Technol.*, 141(3), 031008. DOI: 10.1115/1.4042865.
- [22] Toktaş, S.E. and Dag, S. (2020). Oblique surface cracking and crack closure in an orthotropic medium under contact loading, *Theor. Appl. Fract. Mech.*, 109, 102729. DOI: 10.1016/j.tafmec.2020.102729.
- [23] Lubich, S., Fischer, C., Schilli, S. and Seifert, T. (2022). Microstructure-sensitive finite-element analysis of crack-tip opening displacement and crack closure for microstructural short fatigue cracks, *Int. J. Fatigue*, 162, 106911. DOI: 10.1016/j.ijfatigue.2022.106911.
- [24] Miao, X., Hong, H., Hong, X., Peng, J. and Bie, F. (2022). Effect of constraint and crack contact closure on fatigue crack mechanical behavior of specimen under negative loading ratio by Finite Element Method, *Metals*, 12(11), 1858. DOI: 10.3390/met12111858.
- [25] Elmhaia, O., Belaasilia, Y., Askour, O., Braikat, B. and Damil, N. (2023). Numerical analysis of frictional contact between crack lips in the framework of Linear Elastic Fracture Mechanics by a mesh-free approach, *Theor. Appl. Fract. Mech.*, 124, 103749. DOI: 10.1016/j.tafmec.2023.103749
- [26] Markides, C.F., Papis, D.N. and Kourkoulis, S.K. (2011). Stress intensity factors for the Brazilian disc with a short central crack: Opening versus closing cracks, *Appl. Math. Modell.*, 35(12), pp. 5636-5651. DOI: 10.1016/j.apm.2011.05.013
- [27] Muskhelishvili, N.I. (1953). *Some basic problems of the mathematical theory of elasticity*, Groningen, Noordhoff.
- [28] Markides Ch.F. (2009). PhD Thesis, Mixed mode crack problems and the special case of the cracked Brazilian disc, Supervisor: Papis, D.N., National Technical University of Athens, Athens, Greece.
- [29] Banks-Sills, L. and Arcan, M. (1983). An edge-cracked Mode II fracture specimen: A photoelastic-numerical procedure is used to demonstrate the efficacy of a newly proposed pure-shear fracture specimen, *Exp. Mech.*, 23, pp. 257-261. DOI: 10.1007/BF02319251.
- [30] Banks-Sills, L., Arcan, M. and Bortman, Y. (1984). A mixed mode fracture specimen for mode II dominant deformation, *Eng. Fract. Mech.*, 20(1), 145-157. DOI: 10.1016/0013-7944(84)90122-X.
- [31] Banks-Sills, L., Arcan, M. and Gabay, H. (1984). A mode II fracture specimen - finite element analysis, *Eng. Fract. Mech.*, 19(4), 739-750. DOI: 10.1016/0013-7944(84)90105-X.